

AD-A203 650

DTIC FILE COPY

1

ESL-TR-86-36

SOOT FORMATION BEHIND A BLUFF BODY BURNER

CHARLES L. PROCTOR
ABDERRAHMANE TOUATI

UNIVERSITY OF FLORIDA
COMBUSTION LABORATORY
DEPARTMENT OF
MECHANICAL ENGINEERING
GAINESVILLE, FLORIDA 32611

OCTOBER 1986

FINAL REPORT

MAY 1983 - OCTOBER 1985

DTIC
ELECTE
DEC 12 1988
S D

APPROVED FOR PUBLIC RELEASE; DISTRIBUTION UNLIMITED



AFEGSC

ENGINEERING & SERVICES LABORATORY
AIR FORCE ENGINEERING & SERVICES CENTER
TYNDALL AIR FORCE BASE, FLORIDA 32403

8 8 12 9 052

REPORT DOCUMENTATION PAGE

1a. REPORT SECURITY CLASSIFICATION UNCLASSIFIED			1b. RESTRICTIVE MARKINGS		
2a. SECURITY CLASSIFICATION AUTHORITY			3. DISTRIBUTION/AVAILABILITY OF REPORT Approved for Public Release Distribution Unlimited		
2b. DECLASSIFICATION/DOWNGRADING SCHEDULE					
4. PERFORMING ORGANIZATION REPORT NUMBER(S) ESL-TR-86-36			5. MONITORING ORGANIZATION REPORT NUMBER(S)		
6a. NAME OF PERFORMING ORGANIZATION The University of Florida		6b. OFFICE SYMBOL (If applicable) UFCL	7a. NAME OF MONITORING ORGANIZATION Air Force Engineering and Services Center		
6c. ADDRESS (City, State and ZIP Code) University of Florida Combustion Laboratory Department of Mechanical Engineering Gainesville, Florida 32611			7b. ADDRESS (City, State and ZIP Code) HQ AFESC/RDVS Tyndall AFB, Florida 32403-6001		
8a. NAME OF FUNDING/SPONSORING ORGANIZATION		8b. OFFICE SYMBOL (If applicable)	9. PROCUREMENT INSTRUMENT IDENTIFICATION NUMBER F08635-C-0136, Task 83-03		
8c. ADDRESS (City, State and ZIP Code)			10. SOURCE OF FUNDING NOS.		
			PROGRAM ELEMENT NO.	PROJECT NO.	TASK NO.
			62601F	1900	2059
11. TITLE (Include Security Classification) Soot Formation Behind a Bluff Body Burner					
12. PERSONAL AUTHOR(S) Charles L. Proctor, Abderrahmane Touati					
13a. TYPE OF REPORT Final		13b. TIME COVERED FROM May 83 TO Oct 85		14. DATE OF REPORT (Yr., Mo., Day) October 1986	
				15. PAGE COUNT 48	
16. SUPPLEMENTARY NOTATION Availability of this report is specified on reverse of front cover.					
17. COSATI CODES			18. SUBJECT TERMS (Continue on reverse if necessary and identify by block number)		
FIELD	GROUP	SUB. GR.			
21	05		Soot Formation, Flame Structure, (JF) ←		
21	02		Optical Particle Sizing,		
19. ABSTRACT (Continue on reverse if necessary and identify by block number) The objective of this study was to obtain information on the effects of fuel composition, flame structure on soot formation in a laboratory combustor with turbulent, recirculating flow conditions. Data is to provide a data base on soot formation mechanisms for model development or validation. The report focused on using nonintrusive measurement techniques in turbulent flames without disturbing the flow fields. Particle sizing and population distribution were measured by scattered light intensity ratioing techniques, local flame velocity was measured via laser doppler velocimetry, and temperature measurements were made using Chrome-Alumel thermo couple probes.					
20. DISTRIBUTION/AVAILABILITY OF ABSTRACT UNCLASSIFIED/UNLIMITED <input checked="" type="checkbox"/> SAME AS RPT. <input type="checkbox"/> DTIC USERS <input type="checkbox"/>			21. ABSTRACT SECURITY CLASSIFICATION UNCLASSIFIED		
22a. NAME OF RESPONSIBLE INDIVIDUAL Major Paul E. Kerch			22b. TELEPHONE NUMBER (Include Area Code) (904) 283-4234		22c. OFFICE SYMBOL RDVS

UNCLASSIFIED

SECURITY CLASSIFICATION OF THIS PAGE

UNCLASSIFIED

SECURITY CLASSIFICATION OF THIS PAGE

SUMMARY

This document reports on current research by the University of Florida Combustion Laboratory personel at the Environic's Division Combustion Laboratory and at the University of Florida. The report covers research during the period 10 January 1985 to 30 September 1985. Flames were studied from a non-pre-mixed centerbody type combustor (Figure 1). Particulate sizing and population density measurements were made using light-scattering techniques (Figure 2) in the environsics laboratory. Flame flow-field velocities were measured on the same flames, using a laser doppler velocimeter (Figure 3) at the University of Florida. Very little particle size variations were seen in these flames; however, variation of the operating conditions produced dramatic changes in flame aerodynamic configuration, soot number density, and the location of maximum soot formation.



Accession For	
NTIS CRA&I	<input checked="" type="checkbox"/>
DTIC TAB	<input type="checkbox"/>
Unannounced	<input type="checkbox"/>
Justification	
By	
Distribution/	
Availability Codes	
Dist	Avail and/or Special
A-1	

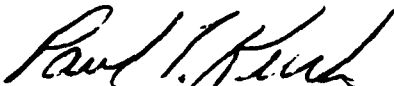
PREFACE


This report was prepared by the University of Florida Combustion Laboratory, Mechanical Engineering Department, Gainesville FL 32611, under Contract Number F08635-C-0136, Task 83-03, for the Air Force Engineering and Services Center, Engineering and Services Laboratory (AFESC/RDVS), Tyndall Air Force Base FL 32403-6001.


This report summarizes work done at the Engineering and Services Laboratory, Environics Division Particle Measurements Laboratory and the University of Florida Combustion Laboratory between 10 January 1985 and 30 September 1985. The HQ AFESC/RDVS project officer was Major Paul E. Kerch.


This report has been reviewed by the Public Affairs Office (PA) and is releasable to the National Technical Information Service (NTIS). At NTIS, it will be available to the general public, including foreign nationals.

This technical report has been reviewed and is approved for publication.


PAUL E. KERCH, Maj, USAF
Project Officer


KENNETH T. DENBLEYKER, Maj, USAF
Chief, Environmental Sciences Branch


THOMAS J. WALKER, Lt Col, USAF, BSC
Chief, Environics Division


LAWRENCE D. HOKANSON, Colonel, USAF
Director, Engineering and Services
Laboratory

v
(The reverse of this page is blank.)

TABLE OF CONTENTS

Section	Title	Page
I	INTRODUCTION.....	1
	A. OBJECTIVE.....	1
	B. BACKGROUND.....	1
	C. SCOPE.....	2
II	EXPERIMENTAL APPROACH.....	3
	A. EXPERIMENT.....	3
	1. Modular Burner.....	3
	2. Integrated Particle Sizing System.....	3
	3. Laser Doppler Velocimeter....	5
	B. MEASUREMENTS.....	5
	C. TEST CONDITIONS.....	8
III	ANALYTICAL RESULTS.....	11
	A. PROPANE FLAMES.....	11
	B. 1-BUTENE FLAMES.....	28
	C. ISOBUTYLENE FLAMES.....	32
IV	SUMMARY AND CONCLUSION.....	44
	A. SUMMARY.....	44
	B. CONCLUSION.....	45
	REFERENCES.....	46

LIST OF FIGURES

Figure	Title	Page
1	Bluff Body Burner.....	4
2	Schematic of the Integrated Particle Sizing System.....	6
3	Optical Configuration of the Laser Doppler Velocimeter.....	7
4	Graph of Normalized Particle Count versus Size.....	8
5	Soot Field Data for a Propane Flame operating at a Global Equivalence Ratio of 0.01 and an Air Velocity of 14 m/s.....	14
6	Propane Flame operating at a Global Equivalence Ratio of 0.01 and an Air Velocity of 14 m/s.....	15
7	Propane Flame operating at a Global Equivalence Ratio of 0.02 and an Air Velocity of 14 m/s.....	17
8	Soot Field Data for a Propane Flame operating at a Global Equivalence Ratio of 0.02 and an Air Velocity of 14 m/s.....	18
9	Propane Flame operating at a Global Equivalence Ratio of 0.03 and an Air Velocity of 14 m/s.....	19
10	Soot Field Data for a Propane Flame operating at a Global Equivalence Ratio of 0.03 and an Air Velocity of 14 m/s.....	20
11	Propane Flame operating at a Global Equivalence Ratio of 0.03 and an Air Velocity of 10 m/s.....	22
12	Propane Flame operating at a Global Equivalence Ratio of 0.03 and an Air Velocity of 12 m/s.....	23
13	Soot Field Data for a Propane Flame operating at a Global Equivalence Ratio of 0.03 and an Air Velocity of 10 m/s.....	25

LIST OF FIGURES
(Continued)

Figure	Title	Page
14	Soot Field Data for a Propane Flame operating at a Global Equivalence Ratio of 0.03 and an Air Velocity of 12 m/s.....	26
15	Axial Flame Velocity Profiles for a Propane Flame operating at a Global Equivalence Ratio of 0.03 and an Air Velocity of 10 m/s.....	26
16	Axial Flame Velocity Profiles for a Propane Flame operating at a Global Equivalence Ratio of 0.03 and an Air velocity of 12 m/s.....	27
17	Axial Flame Velocity Profiles for a Propane Flame operating at a Global Equivalence Ratio of 0.03 and an Air Velocity of 14 m/s.....	28
18	Radial Flame Velocity Profiles for a Propane Flame operating at a Global Equivalence Ratio of 0.03 and an Air Velocity of 10 m/s.....	30
19	Radial Flame Velocity Profiles for a Propane Flame operating at a Global Equivalence Ratio of 0.03 and an Air Velocity of 12 m/s.....	31
20	Radial Flame Velocity Profiles for a Propane Flame operating at a Global Equivalence Ratio of 0.03 and an Air Velocity of 14 m/s.....	32
21	Temperature Profiles for a Propane Flame operating at a Global Equivalence Ratio of 0.03 and an Air Velocity of 10 m/s.....	33
22	Temperature Profiles for a Propane Flame operating at a Global Equivalence Ratio of 0.03 and an Air Velocity of 12 m/s.....	34
23	Temperature Profiles for a Propane Flame operating at a Global Equivalence Ratio of 0.03 and an Air Velocity of 14 m/s.....	35
24	Soot Field Data for 1-Butene Flame operating at a Global Equivalence Ratio of 0.03 and an Air Velocity of 14 m/s.....	37
25	Soot Field Data for 1-Butene Flame operating at a Global Equivalence Ratio of 0.04 and an Air Velocity of 14 m/s.....	38

LIST OF FIGURES
(Concluded)

Figure	Title	Page
26	Soot Field Data for 1-Butene Flame operating at a Global Equivalence Ratio of 0.05 and an Air Velocity of 14 m/s.....	39
27	Soot Field Data for 1-Butene Flame operating at a Global Equivalence Ratio of 0.03 and an Air Velocity of 12 m/s.....	41
28	Soot Field Data for 1-Butene Flame operating at a Global Equivalence Ratio of 0.03 and an Air Velocity of 18 m/s.....	42
29	Soot Field Data for an Isobutylene Flame operating at a Global Equivalence Ratio of 0.03 and an Air Velocity of 10 m/s.....	43
30	Soot Field Data for an Isobutylene Flame operating at a Global Equivalence Ratio of 0.03 and an Air Velocity of 12 m/s.....	44
31	Soot Field Data for an Isobutylene Flame operating at a Global Equivalence Ratio of 0.03 and an Air Velocity of 14 m/s.....,.....	45
32	Soot Field Data for an Isobutylene Flame operating at a Global Equivalence Ratio of 0.04 and an Air Velocity of 14 m/s.....	47
33	Soot Field Data for an Isobutylene Flame operating at a Global Equivalence Ratio of 0.05 and an Air Velocity of 14 m/s.....	48

SECTION I

INTRODUCTION

A. OBJECTIVE

The objective of this work is to investigate several key parameters that affect soot formation and oxidation in practical combustors. Recognizing the difficulties encountered in modeling turbulent flames, this study is expected to elucidate some aspects of the soot production processes and to provide a data base for model development or validation of existing models (References 1-2).

This effort is concerned with the effects of molecular structure, flame aerodynamics, and temperature on the soot field of axisymmetric turbulent diffusion flames with recirculating flow fields.

B. BACKGROUND

The gradual broadening of the composition of military aircraft fuels can cause an increase in soot production and emissions. Such an increase can hinder the performance of combustion engines and increase soot emissions to the atmosphere which can be hazardous to human health and degrade the quality of the environment. Stricter environmental regulations and the need for more efficient engines makes soot-related research necessary.

Soot production in practical combustors involves several complex processes such as flame aerodynamics, heat transfer, and chemistry. These processes are interrelated and depend on the combustor design and operating conditions. The choice of a combustor type and operating conditions can establish the relative importance of these processes. Turbulent diffusion flames are an important class of practical flames where the combustion process is mixing-controlled. Gas turbine engines, in general, operate under the turbulent diffusion flame concept.

SCOPE

This research effort focussed on using and developing nonintrusive measurement techniques capable of providing real-time data acquisition in turbulent flames without disturbing the flow fields. Laser doppler velocimetry and scattered light intensity-ratioing techniques were used to measure local flame velocity and soot particulate size and population distribution, respectively. Temperature measurements were made using chromel-alumel thermocouple probes.

The effects of flame aerodynamics, temperature, global equivalence ratio, and fuel structure on the soot field in these flames were investigated. Insights into soot particle behavior in these flames were pursued.

SECTION II

EXPERIMENTAL APPROACH

A. EXPERIMENT

1. Modular burner

The burner used for the current study is a non-pre-mixed centerbody combustor exhausting into free air. Studies on this type of combustor were initiated by the Air Force Wright Aeronautical Laboratories/Aeropropulsion laboratory (Reference 3). Through variation of the operating conditions, this type of burner can generate turbulent diffusion flames of variable flow configuration and stability (Reference 4).

The burner used in this study consists of a central fuel jet surrounded by an annular air jet (Figure 1). The air flow enters the annular passage, passes through a flow straightener, and exhausts at the burner exit plane. The outer air passage has a 3.175-inch inside diameter while the centerbody has a 2.25-inch outside diameter. The fuel jet passes through a tube in the centerbody and exits through a 0.054-inch diameter nozzle. Compressed air, relatively free of contamination by particles, water, and oil droplets, was supplied to a plenum chamber surrounding the central fuel jet.

2. Integrated Particle Sizing System.

In situ particle size and population measurements in flames are used in combustion research (References 5-7). Knowledge of the path followed by a soot particle and its evolution in a particular flow field is essential for understanding the formation, growth, and destruction processes of soot.

This study involves an optical probe capable of performing nonintrusive, in situ, real-time point measurements of soot size and population distribution in a flame. This probe is based on the scattered light intensity ratioing technique (Reference 8). To use this technique, one measures the intensity of the forward scattered light by soot particles passing at the probe volume at two off-axis angles. The ratio of the collected intensities is then processed by a ratio processor. The measured intensity ratio is then reduced to size via comparisons with tabulated values of intensity ratios versus size obtained from Mie scattering theory for spherical particles of arbitrary size and known index of refraction (References 9-11).

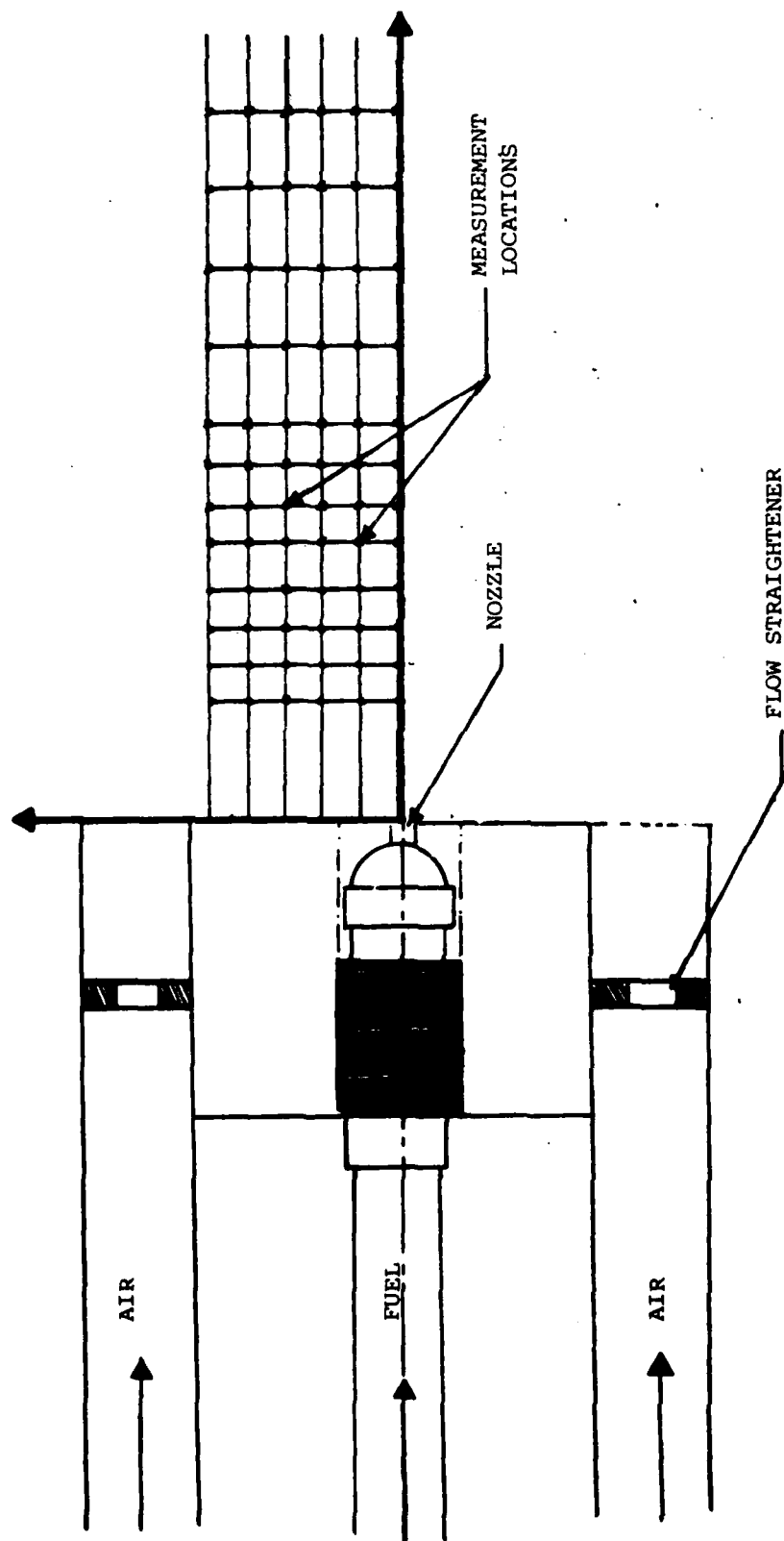


Figure 1. Bluff Body Burner

The large-angle (40° , 20°) receiving optics was used in this study to provide point measurements of soot particle size and population density distribution in the particle size range of 0.12 to 0.57 micrometers. A schematic of the optical system is shown in Figure 2. The incident radiation is supplied by the 488 nanometer line of a 2-watt Lexel argon-ion laser operating in the multiline mode.

3. Laser Doppler Velocimeter.

The laser doppler velocimeter (LDV) used in this study is a high-power dual-beam configuration with frequency shifting. It consists of a 4-watt Lexel argon-ion laser and a TSI Inc. modified back scattered 9100-6 modular optical assembly. The optical configuration of the LDV is shown in Figure 3. The system uses submicrometer aluminum oxide particles for seeding.

B. MEASUREMENTS

The integrated particle sizing system, at Tyndall AFB, was used to map flames for soot particle size and population density. Radial profiles of soot size and population density were obtained with this optical system for three fuels (propane, 1-butene, and isobutylene). Temperature measurements were taken with an insulated chromel-alumel probe mounted on a rigid support. Velocities were determined, at the University of Florida, using the laser doppler velocimeter at the same locations where the soot particle size and population density measurements were taken. The measured data are presented for 82 axial/radial locations. These locations are nondimensionalized to the radius ($R = 1.125$ inches) of the bluff body combustor. The relative soot particle data rate for each flame is normalized to the highest data rate, N_1 , found in the flame itself.

Because of the high soot particle density produced in flames using 1-butene and isobutylene fuels, the signals sent to the ratio processor from the photomultiplier tubes could not be processed fast enough for representative measurements of soot size and population density. A signal can be processed only when the peak of the preceding signal decays 1 volt. When high number density signals are sent to the ratio processor the time lapse between two consecutive signals is too small to allow the intensity of the first signal to decay 1 volt. This prevents subsequent signals from being processed.

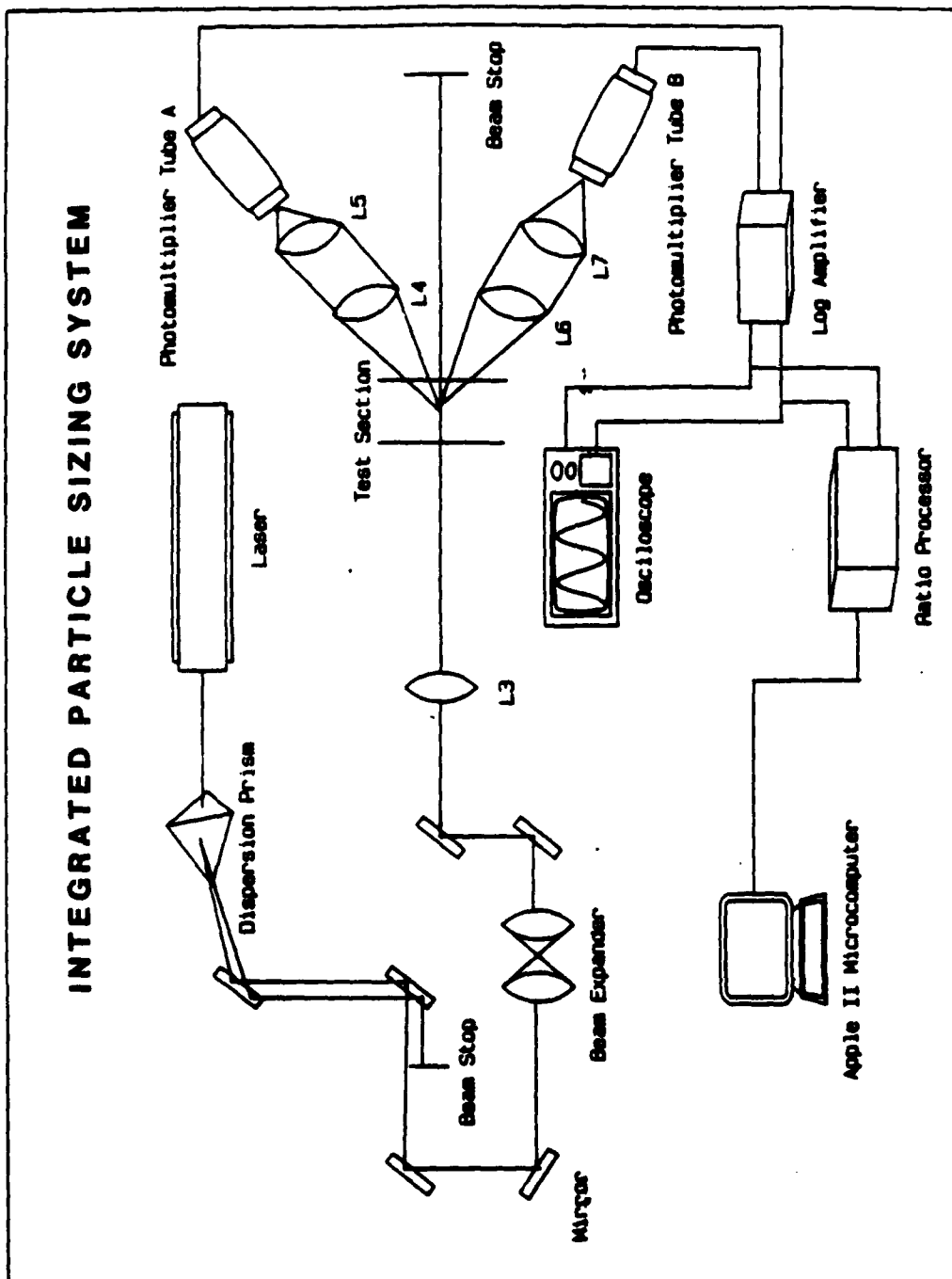


Figure 2. Schematic of the Integrated Particle Sizing System

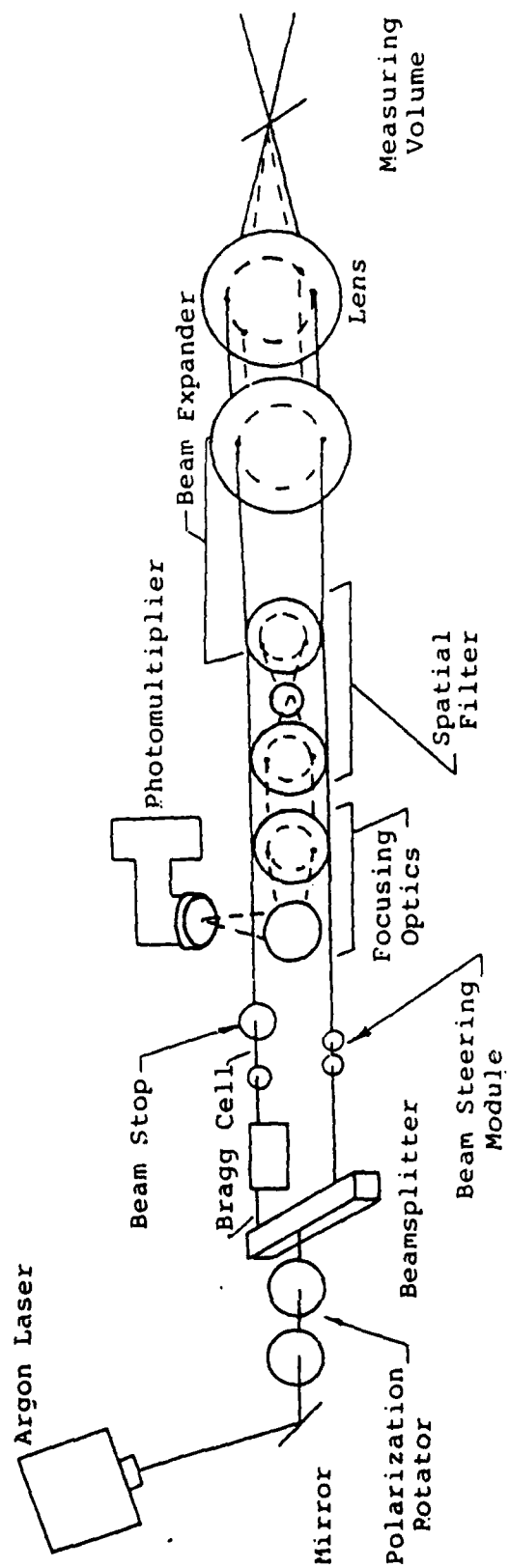


Figure 3. Optical Configuration of the Laser Doppler Velocimeter

A mask with a 1/2-inch diameter hole at the center was placed on each set of receiving lenses. The above adjustment reduced the probe volume size which, in turn, caused fewer signals to be processed. This allowed the signals to be processed individually.

Reduction of the area of the receiving lenses by masking them reduces the measured count rate. However, this study was intended to establish the different regions of importance in the soot field and how they are affected by the combustor operating conditions. An absolute measure of the soot number density, although needed to quantify the sooting propensity of a particular fuel, is not necessary in this work. The normalized count rates are reported here to eliminate the effect of reducing the areas of the receiving lenses on the results.

The effects of the masks placed on the receiving lenses are illustrated in Figures 4a and 4b for a point inside a propane flame. The measurements of soot size and population density were taken consecutively, with and without masks, on the receiving lenses. As expected, the measured particle count rate dropped dramatically because of the reduction of the area of the receiving lenses. A small portion of the smaller particle size of the distribution was cut. This is probably due to the Gaussian nature of the beam or to a small difference in the diameter of the holes when they were made.

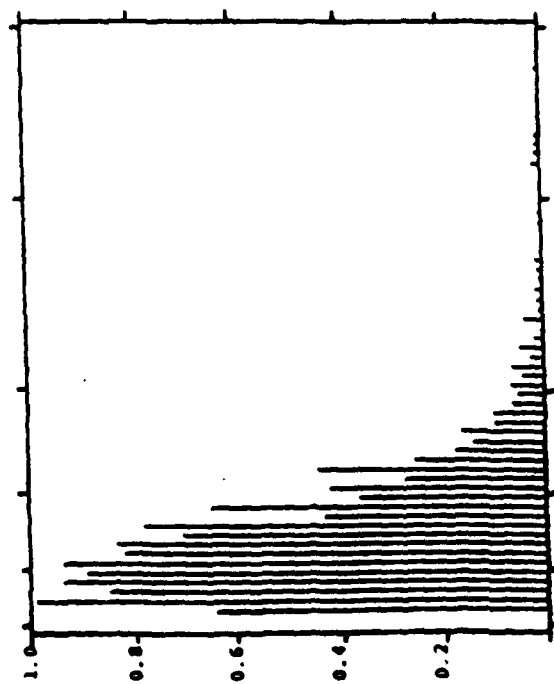
C. TEST CONDITIONS

A test matrix for the different operating conditions is presented in Table 1. The first set of experiments consisted of testing each fuel at three overall fuel-to-air equivalence ratios at a fixed-reference air velocity. The three equivalence ratios were chosen to produce three categories of flames: a highly recirculating and stable flame, an unstable flame in a transitional state, and a stable, weak recirculating flame. The flame varied from a cylindrical to a conical shape as the fuel flow rate was increased and the air velocity was held constant.

The second set of experiments consisted of investigating the flame-scaling effect on the soot field. The global equivalence ratio was maintained constant while the fuel and air flow rates were varied.

Date: 09/27/85
 Series: C3H8 Run: Test
 Comment: Test without mask on the
 receiving lenses

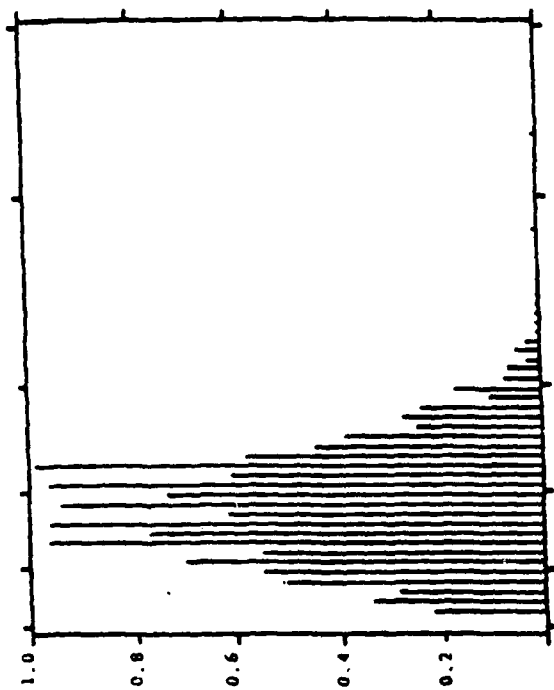
MAX RAW COUNT = 152
 TOTAL RAW COUNT = 1936
 SAMPLE TIME: 8.25 SECONDS



(a)

Date: 09/27/85
 Series: C3H8 Run: Test Mask
 Comment: Test with mask on the
 receiving lenses

MAX RAW COUNT = 152
 TOTAL RAW COUNT = 2078
 SAMPLE TIME: 200.0 SECONDS



(b)

Figure 4a&b. Graph of Normalized Particle Count versus Particle Size

TABLE 1. OPERATING CONDITIONS

<u>FLAME</u>	<u>FUEL</u>	<u>EQUIVALENCE RATIO</u>	<u>AIR REFERENCE VELOCITY</u> m/s
P1	PROPANE	0.01	14
P2	PROPANE	0.02	14
P3	PROPANE	0.03	14
P11	PROPANE	0.03	10
P22	PROPANE	0.03	12
P33	PROPANE	0.03	14
B1	1-BUTENE	0.03	14
B2	1-BUTENE	0.04	14
B3	1-BUTENE	0.05	14
B11	1-BUTENE	0.03	12
B22	1-BUTENE	0.03	14
B33	1-BUTENE	0.03	18
I1	ISOBUTYLENE	0.03	14
I2	ISOBUTYLENE	0.04	14
I3	ISOBUTYLENE	0.05	14
I11	ISOBUTYLENE	0.03	10
I22	ISOBUTYLENE	0.03	12
I33	ISOBUTYLENE	0.03	14

SECTION III

ANALYTICAL RESULTS

A. PROPANE FLAME

This section discusses propane flames in relation to the parameters that affect the soot field. The number mean diameter of the soot particles was found to remain constant ($NMD = 0.27$) when changing the flow conditions. Although changes in diameter of the particles were observed throughout the flames, these changes did not exceed the standard deviation calculated for each point measurement (about 0.07 micrometers).

The soot particle number density was found to be the most dependent on flow conditions. Similar observations on the effects of flow conditions on particle size and population density were reported (Reference 12).

The relationship between flame aerodynamics and soot field was studied using the three flames (P1, P2, P3) operating, respectively, at an equivalence ratio of 0.01, 0.02, and 0.03. The reference air velocity was set to 14 m/s. An annular region of maximum soot particle population density was observed in all three flames.

Figure 5 presents the soot field data for the highly recirculating flame (P1). In this flame, the reverse flow opposed the fuel jet and spread it outwardly in the radial direction. The flame was cylindrical with a base of the order of the bluff body burner (Figure 6). The region of maximum soot population density was located in the recirculation zone between the fuel jet and the boundary of the annular air flow. Within this region large eddy-like structures were produced as a result of the recirculation. Magnussen (Reference 13) argues that soot is formed and contained in these eddies separated by other regions with little or no soot. The combustion of the soot proceeds from the boundary of the eddies as it is being formed inside the eddies.

A change in the flame configuration was observed as the fuel flow rate was increased to be comparable to the reverse air flow (Figure 7). This produced a metastable flame (P2) in a transitional state. Figure 8 shows the soot field for this flame. There is no defined region of maximum soot population density because of the instability of the flame.

A further increase in the fuel flow rate resulted in a more dramatic change in the flame configuration. This produced a more conical flame (P3) in which the fuel jet

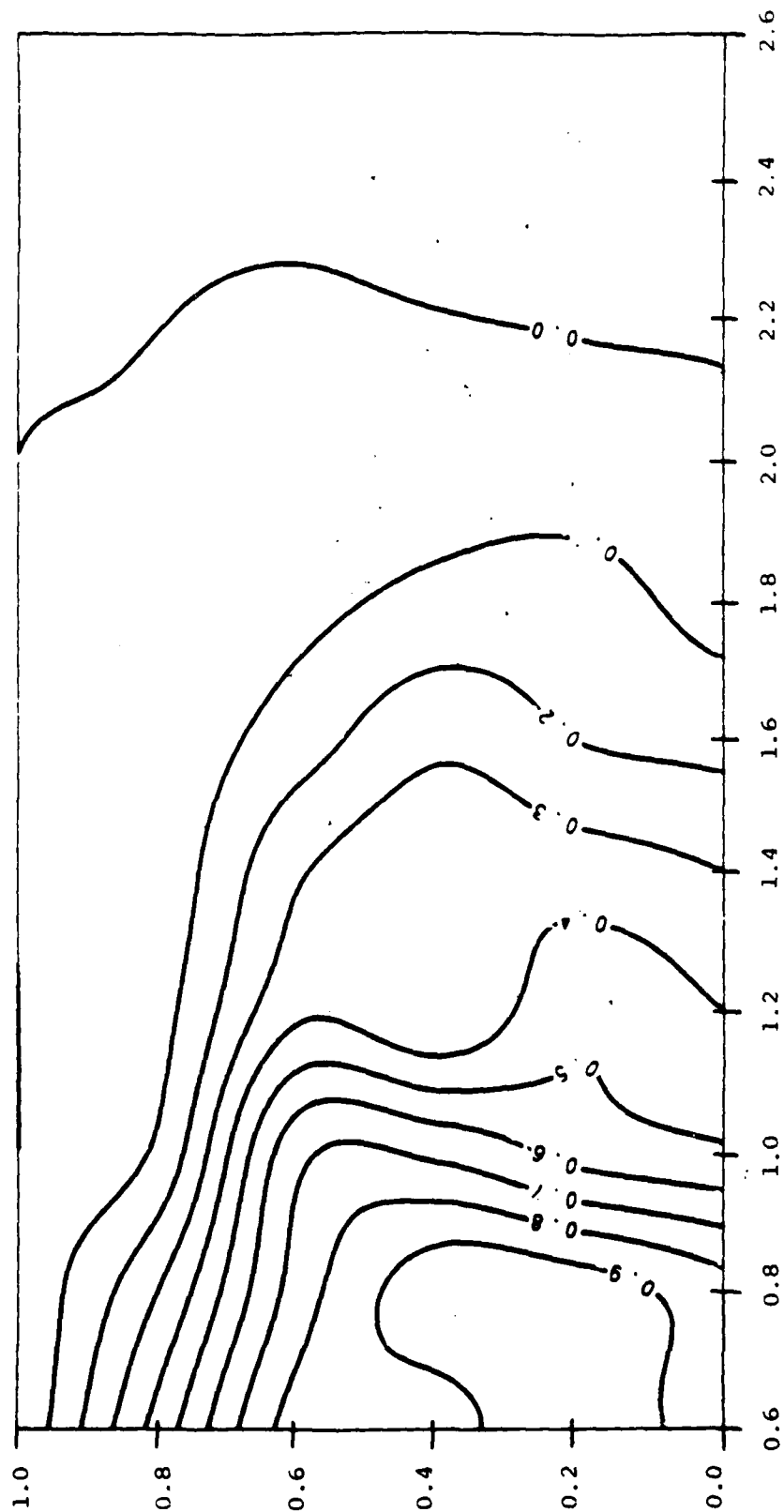


Figure 5. Soot Field Data for a Propane Flame Operating at a Global Equivalence Ratio of 0.01 and an Air Velocity of 14 m/s. (The Isoplots are N/N_1 where $N_1 = 255$ counts/s.)

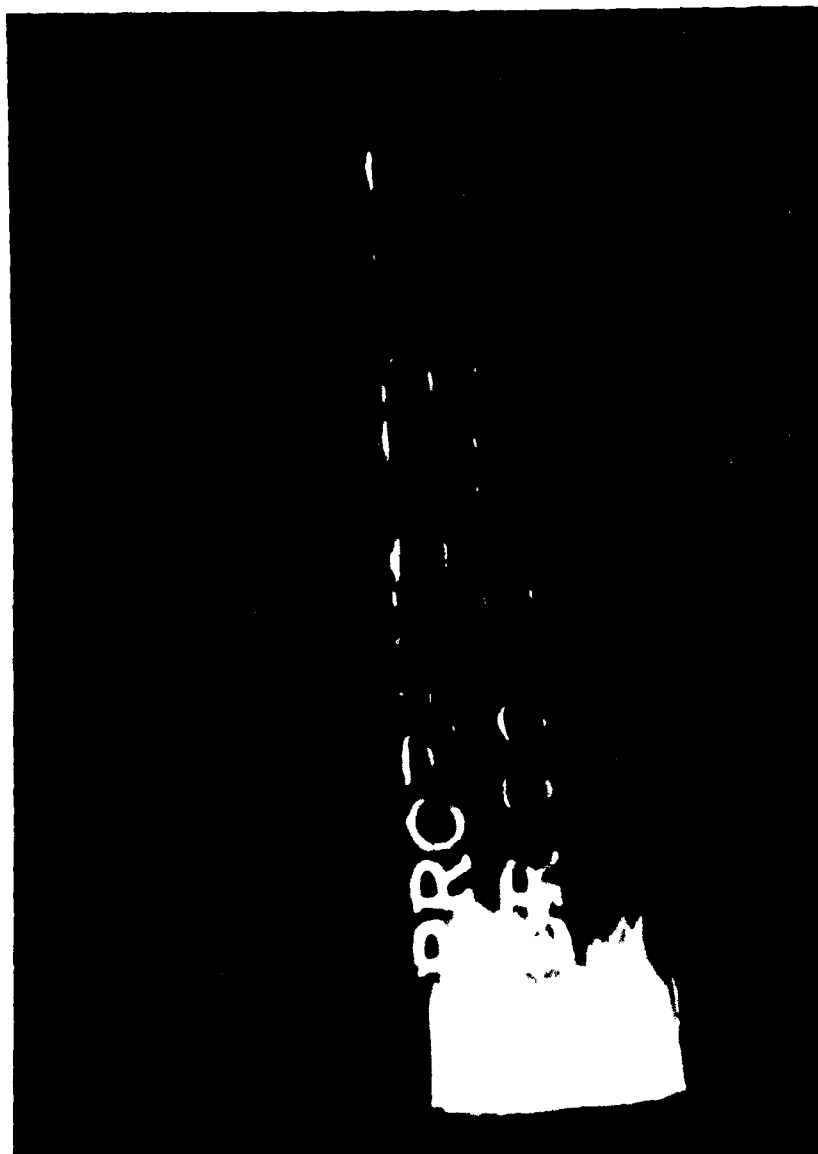


Figure 6. Propane Flame operating at a Global Equivalence ratio of 0.01 and an Air Velocity of 14 m/s.



Figure 7; Propane Flame Operating at a Global Equivalence Ratio of 0.02 and an Air Velocity of 14 m/s.

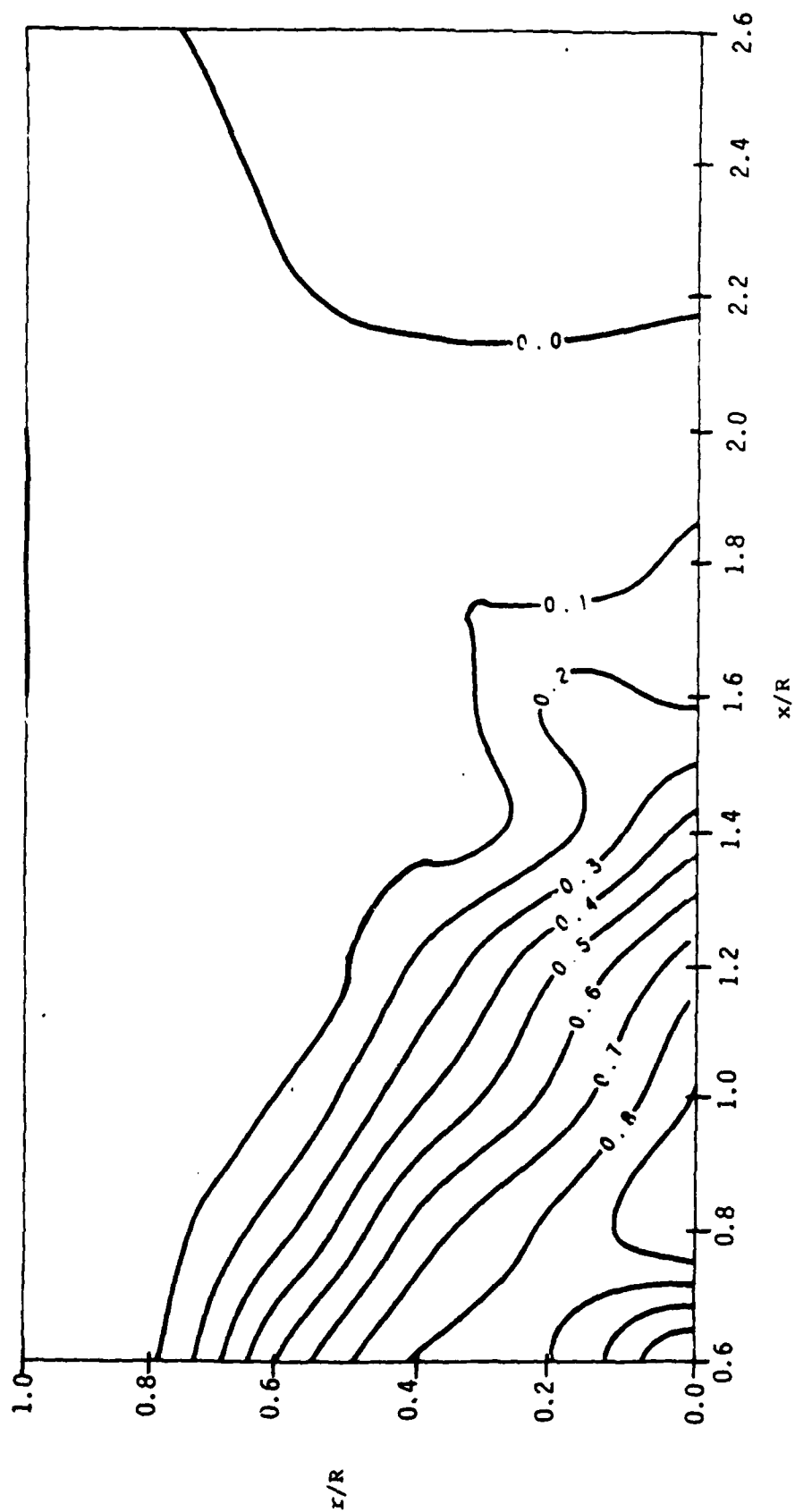


Figure 8. Soot Field Data for a Propane Flame Operating at a Global Equivalence Ratio of 0.02 and an Air velocity of 14 m/s. (The Isoplots are N/N_1 where $N_1 = 228$ counts/s.)

penetrated the recirculation zone completely (Figure 9). A higher soot particle count was measured inside this flame and an axial displacement toward the face of the burner was observed for the region of maximum soot population density (Figure 10). The decay of the soot particle increased with the fuel flow rate. Such an increase in the fuel flow rate might have reduced the vortices between the big eddies and increased the rate of mixing within these eddies. The flame length was found to vary proportionally to the fuel flow rate. The latter observation was previously reported (Reference 14-15), and is predicted (Reference 16) for a laminar diffusion flame.

The flame-scaling effect on soot field was studied, using three propane flames P11, P22, and P33 (Table 1). These flames were operated respectively, at air reference velocities of 10 m/s, 12 m/s, and 14 m/s with an equivalence ratio of 0.03. As the fuel and air flow rates were increased, the length of the flame remained almost constant (Figure 11, 12, and 9) and the thickness of the flame was found to increase with flow conditions. The soot field data shown in Figures 13, 14, and 10 for the three flames show more outward diffusion of the soot particles as the fuel and air flow rates were increased. Further, the decay of the soot population density was more rapid as a result of better mixing in the large scale flame.

Radial and axial velocities for the three flames P11, P22, and P33 were taken at the same locations where soot measurements were made. Strong fluctuations of the flame velocities due mainly to the unsteadiness of the flow field, were observed. Although the velocities measured in these flames are time-averaged quantities, they are very important in the interpretation of the relationship between the flow field and the soot field of a particular flame.

The axial velocity profiles for the three flames studied are shown in Figures 15 through 17. An increase of the flow conditions resulted in an increase of the axial velocity at the centerline. Consequently, a decrease of the vortices between the large eddies and an increase of the rate of mixing within these eddies occurred. This, explains the more rapid decay of the soot particles in the oxidation zone when the flow conditions were increased.

The radial velocity profiles of the three propane flames are shown in Figures 18, 19, and 20, respectively. A radial diffusion of air toward the fuel zone, near the base of the flame was observed when the fuel and air flow rates were increased. Glassman and Yaccarino (Reference 14) hypothesize that, when the oxygen in air enters the fuel zone, the pyrolysis process would be catalysed and higher

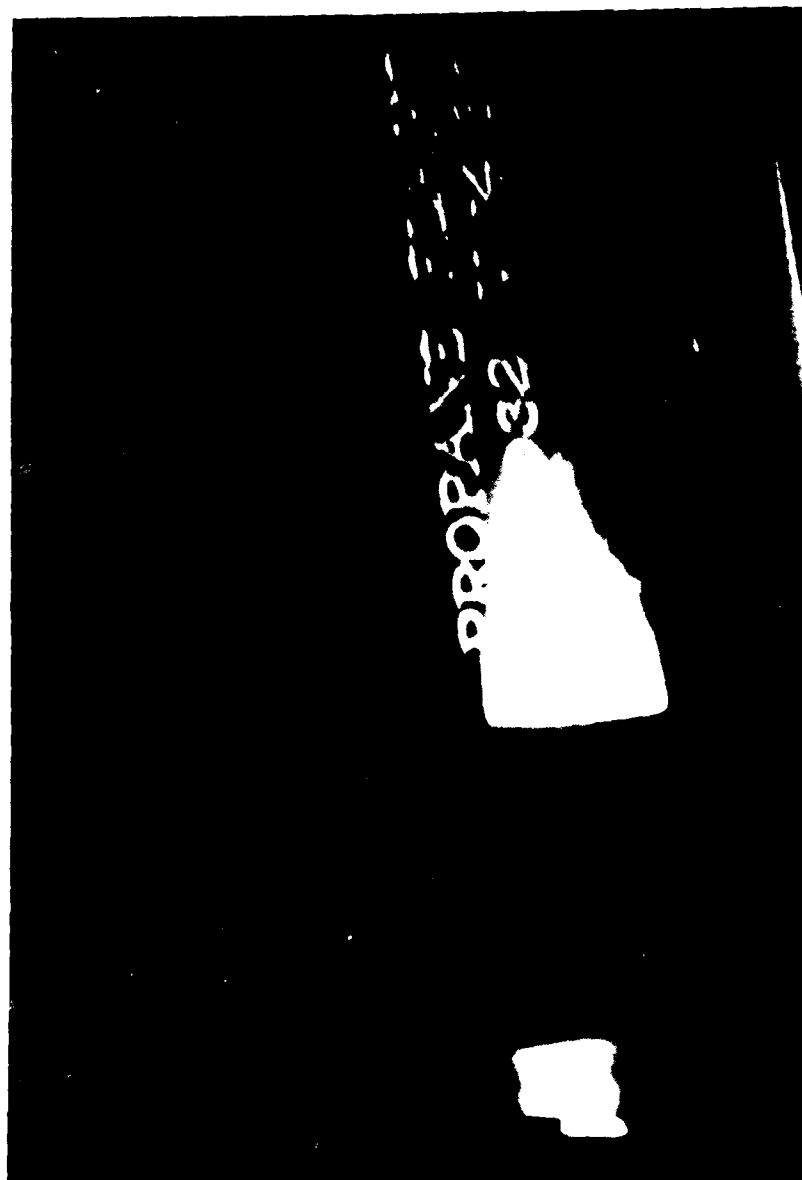


Figure 9. Propane Flame Operating at a Global Equivalence Ratio of 0.03 and an Air Velocity of 14 m/s.

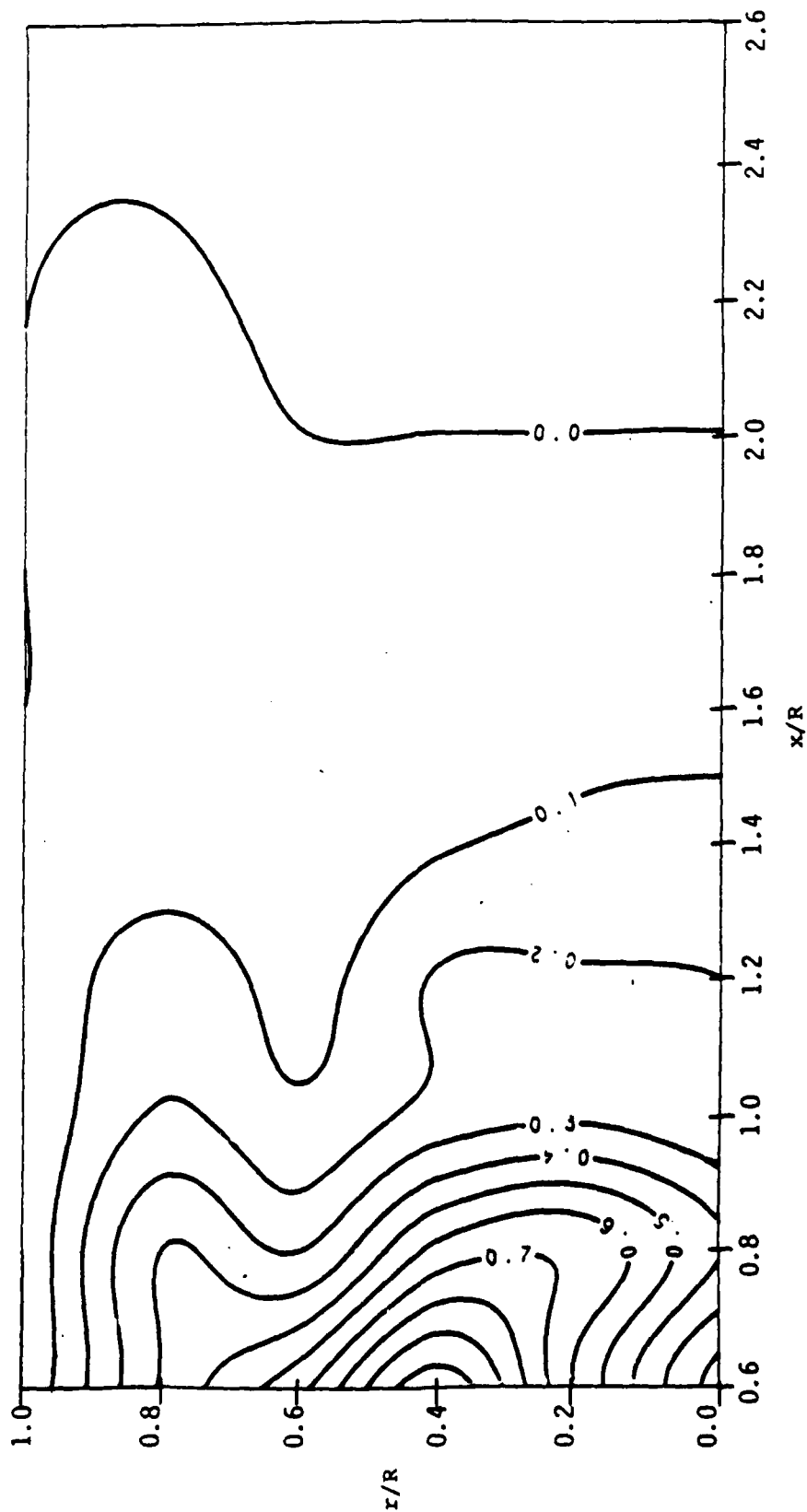


Figure 10. Soot Field Data for a Propane Flame Operating at a Global Equivalence Ratio of 0.03 and an Air Velocity of 14 m/s. (The isoplots are N/N_1 where $n_1 = 592$ counts/s.)



Figure 11. Propane Flame Operating at a Global Equivalence Ratio of 0.03 and an Air Velocity of 10 m/s.

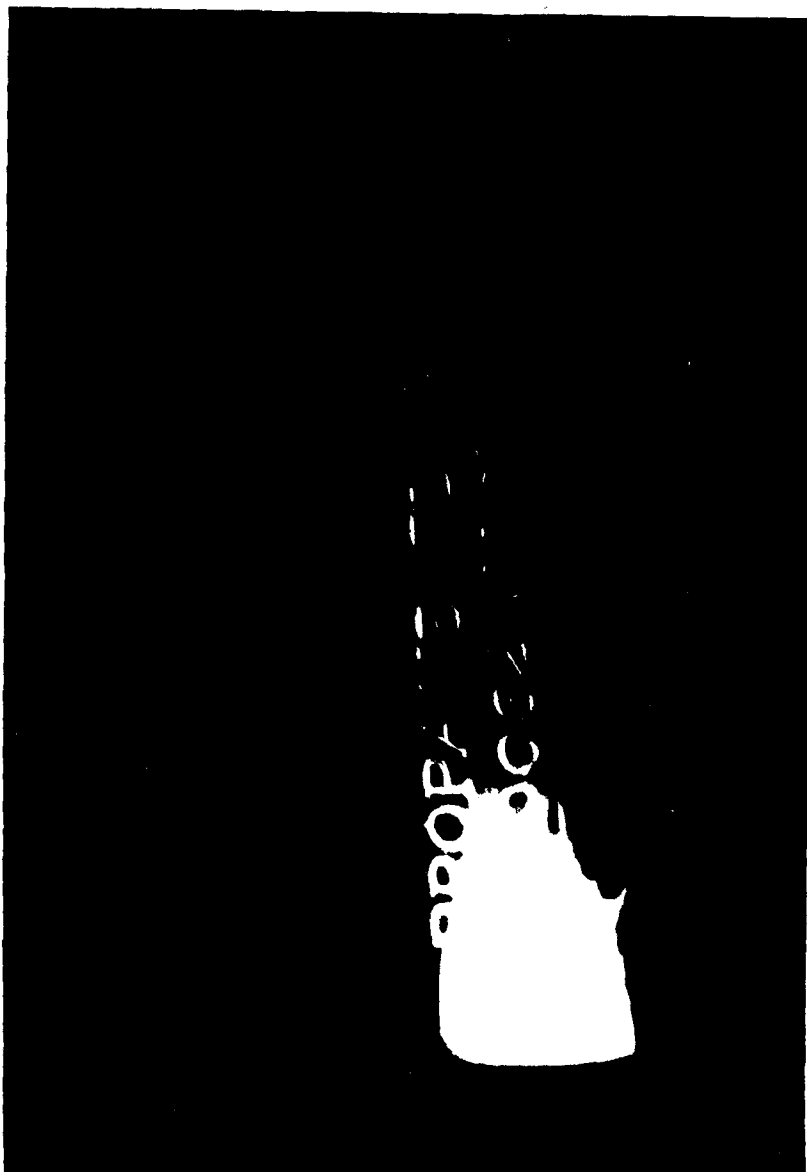


Figure 12. Propane Flame Operating at a Global Equivalence Ratio of 0.03 and an Air Velocity of 12 m/s.

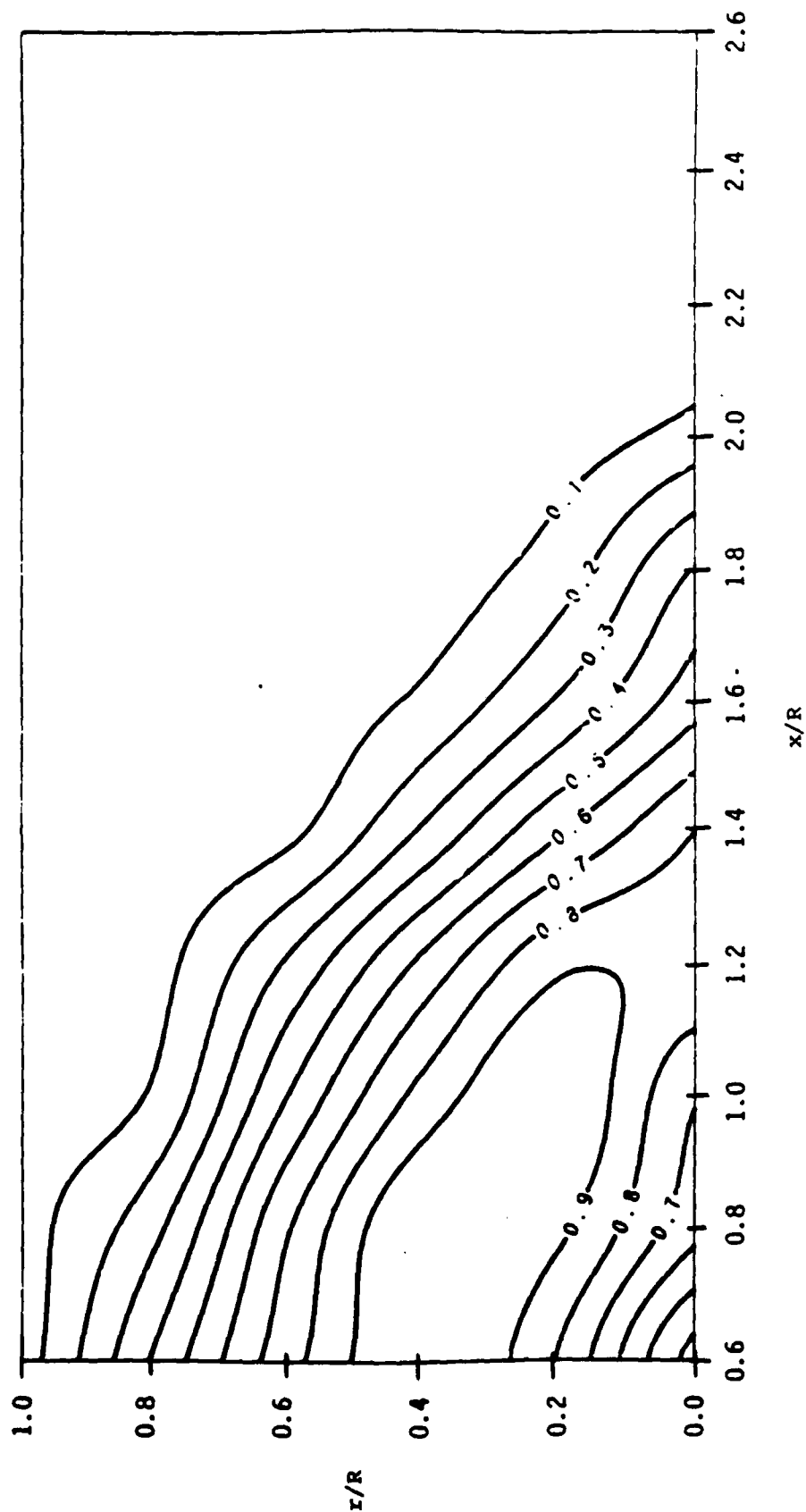


Figure 13. Soot Field Data for a Propane Flame Operating at a Global Equivalence Ratio of 0.03 and an Air Velocity of 10 m/s. (The Isoplots are N/N_1 where $N_1 = 418$ counts/s.

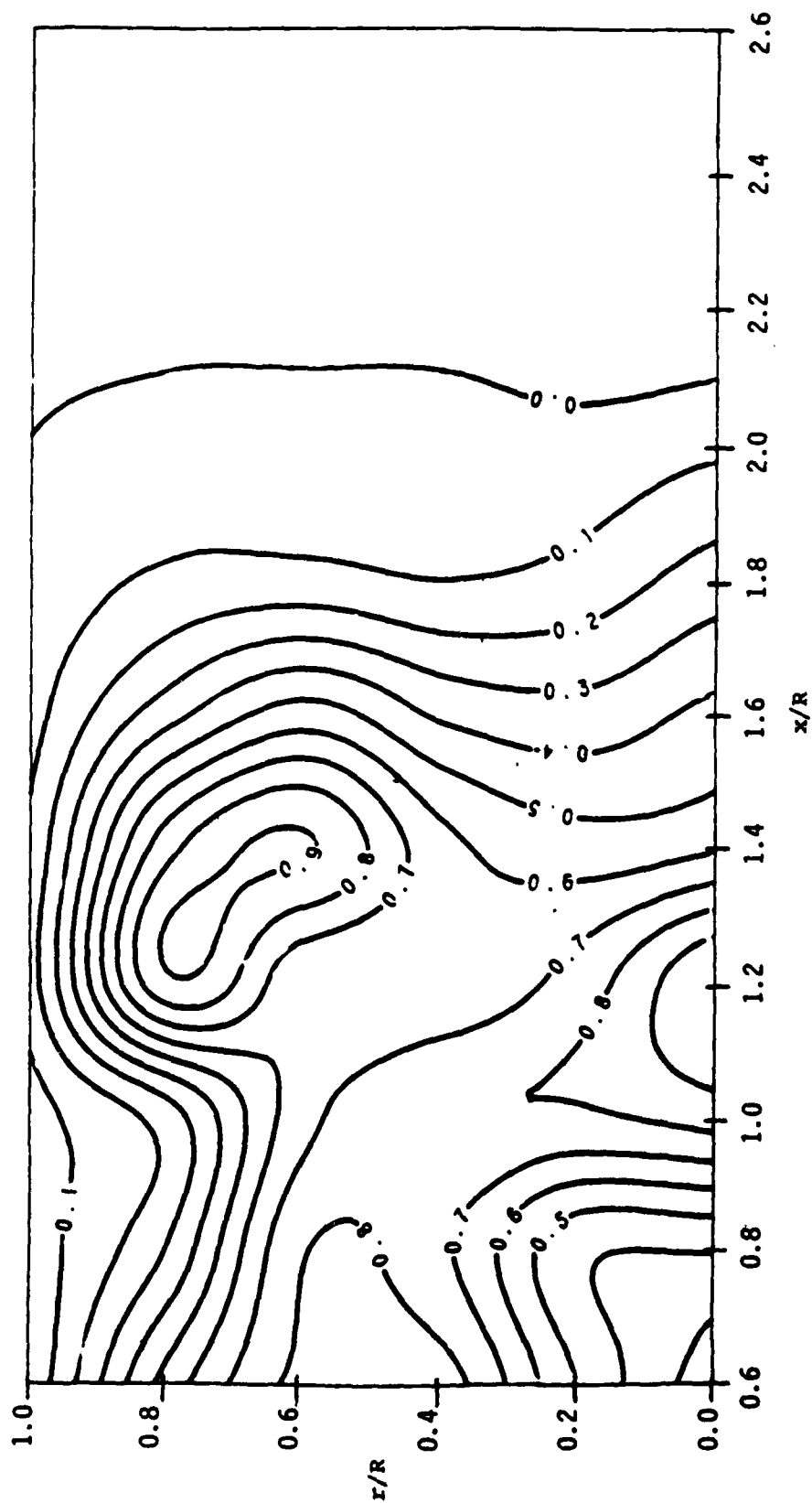


Figure 14. Soot Field Data for a Propane Flame Operating at a Global Equivalence Ratio of 0.03 and an Air Velocity of 12 m/s. (The Isoplots are N/N_1 where $N_1 = 480$ counts/s.)

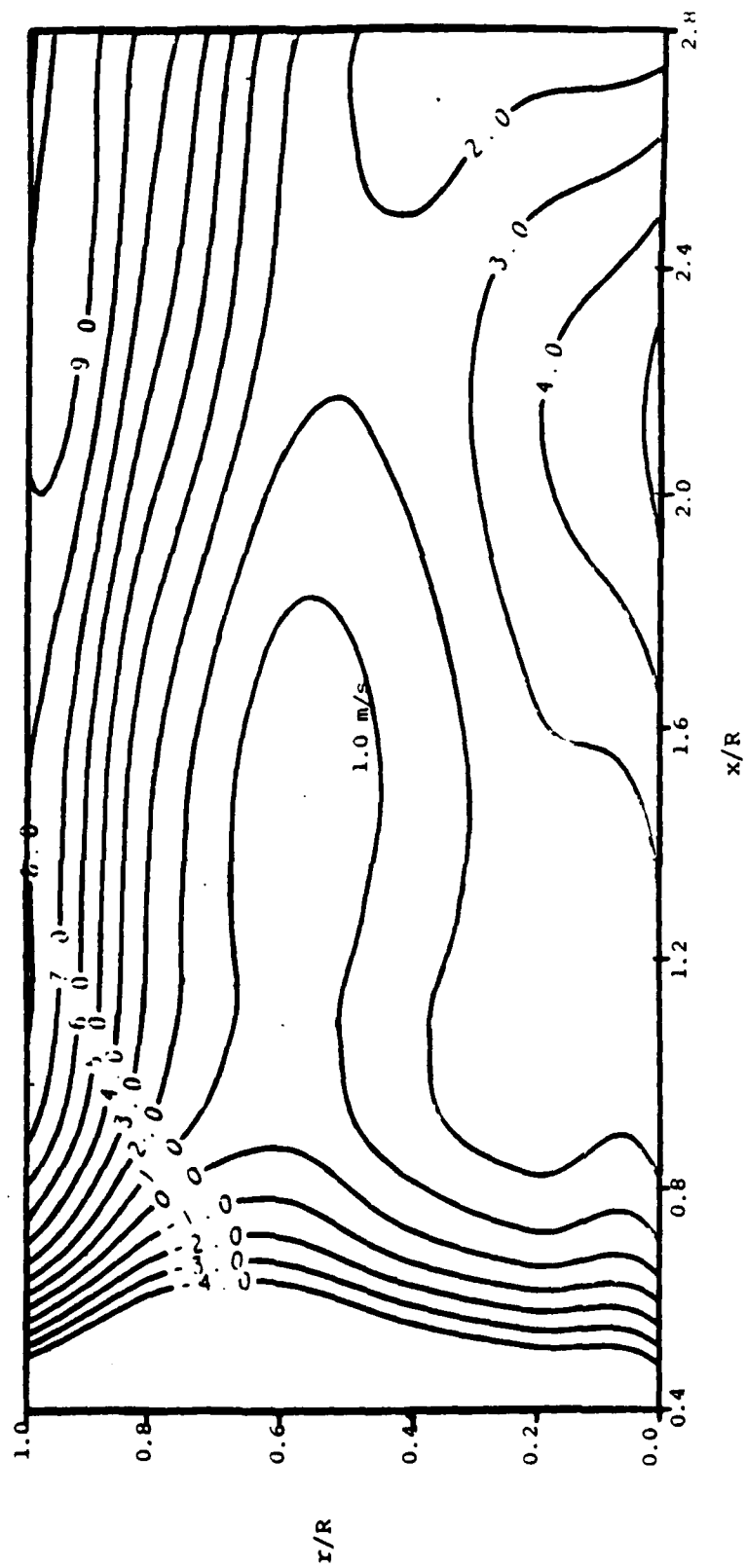


Figure 15. Axial Flame Velocity Profiles for a Propane Flame Operating at a Global Equivalence Ratio of 0.03 and an Air Velocity of 10 m/s.

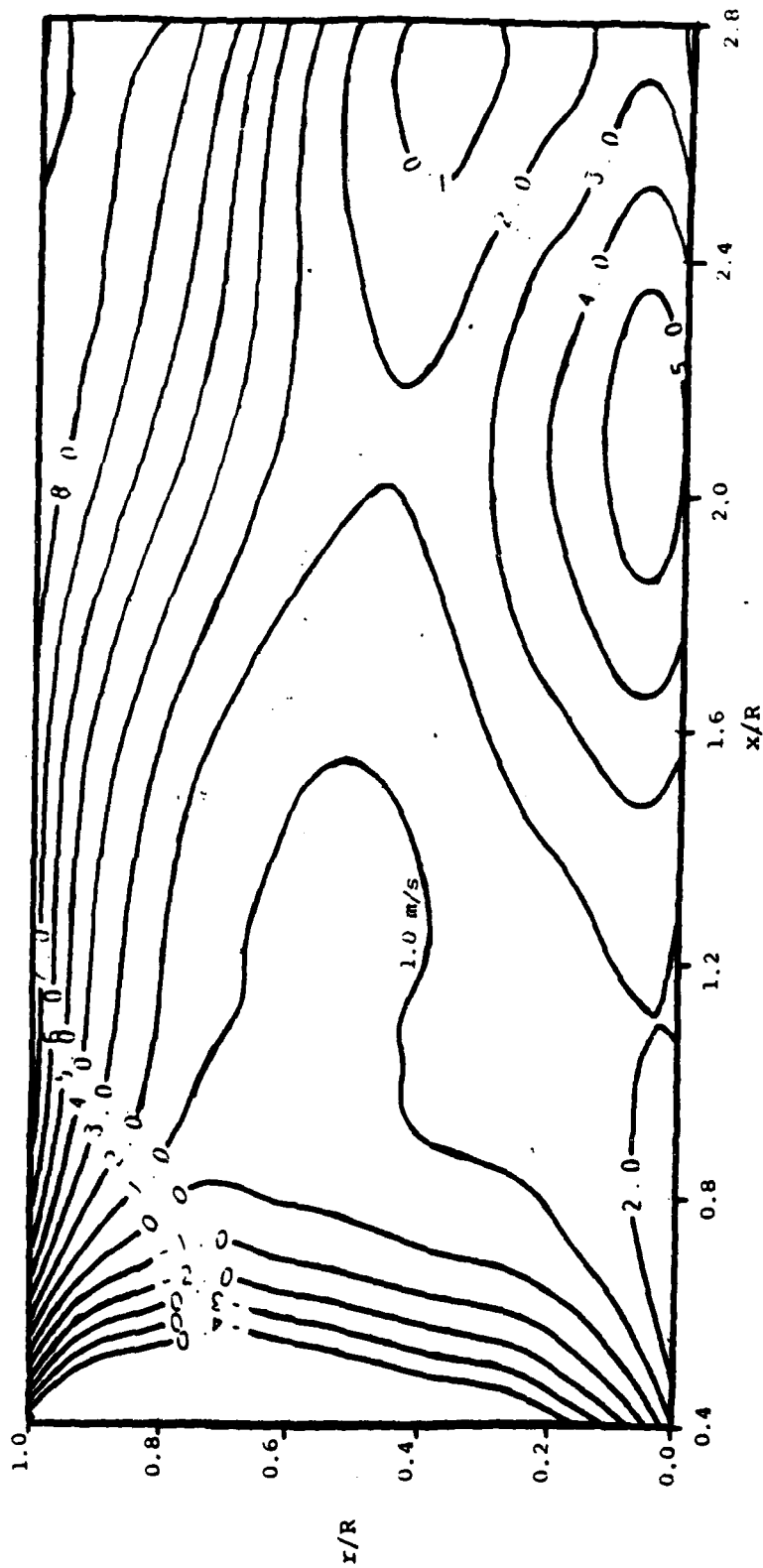


Figure 16. Axial Flame Velocity Profiles for a Propane Flame Operating at a Global Equivalence Ratio of 0.03 and an Air Velocity of 12 m/s.

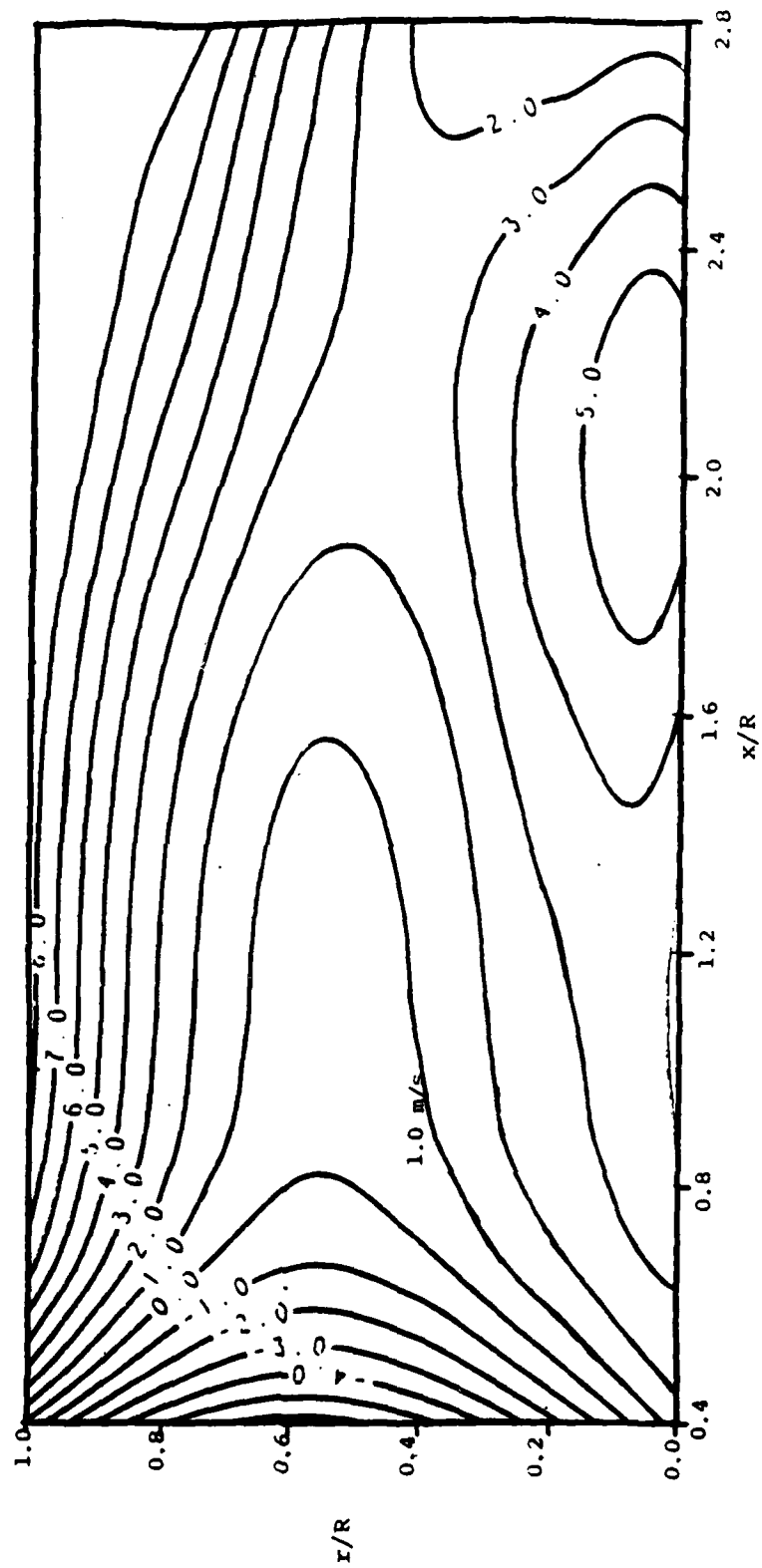


Figure 17. Axial Flame Velocity Profiles for a Propane Flame Operating at a Global Equivalence Ratio of 0.03 and an Air Velocity of 14 m/s.

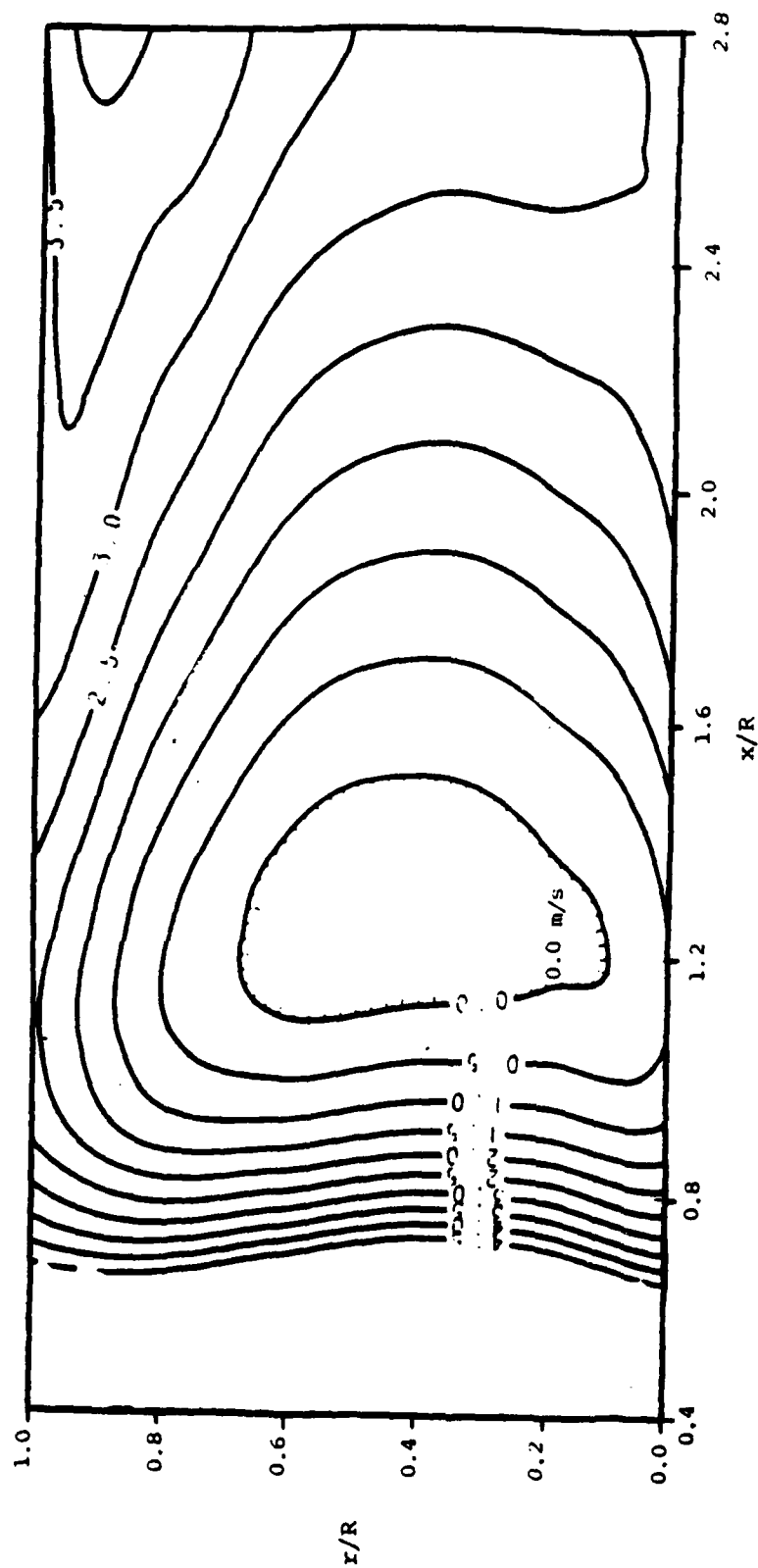


Figure 18. Radial Flame Velocity Profiles for a Propane Flame Operating at a Global Equivalence Ratio of 0.03 and an Air Velocity of 10 m/s.

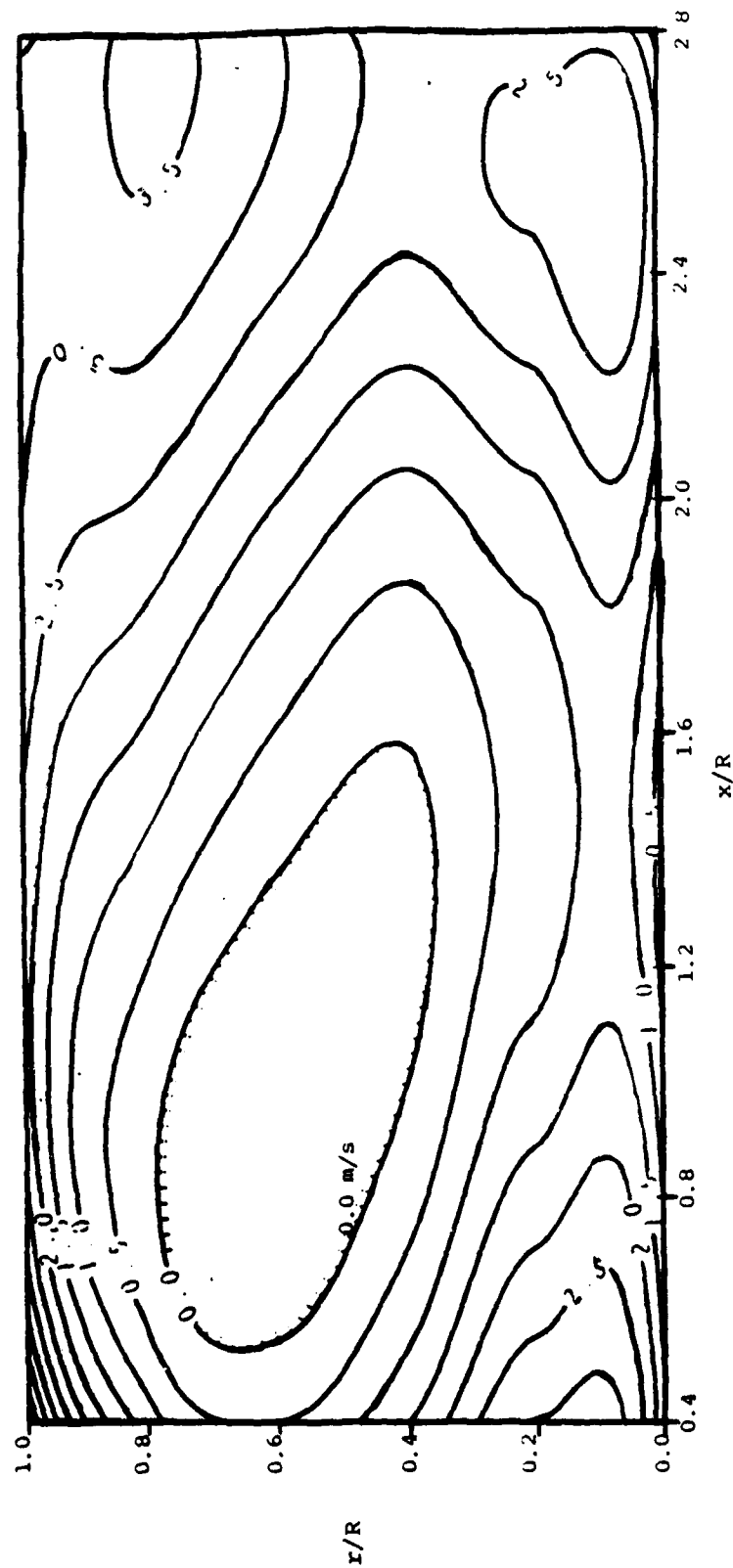


Figure 19. Radial Flame Velocity Profiles for a Propane Flame Operating at a Global Equivalence Ratio of 0.03 and an Air Velocity of 12 m/s.

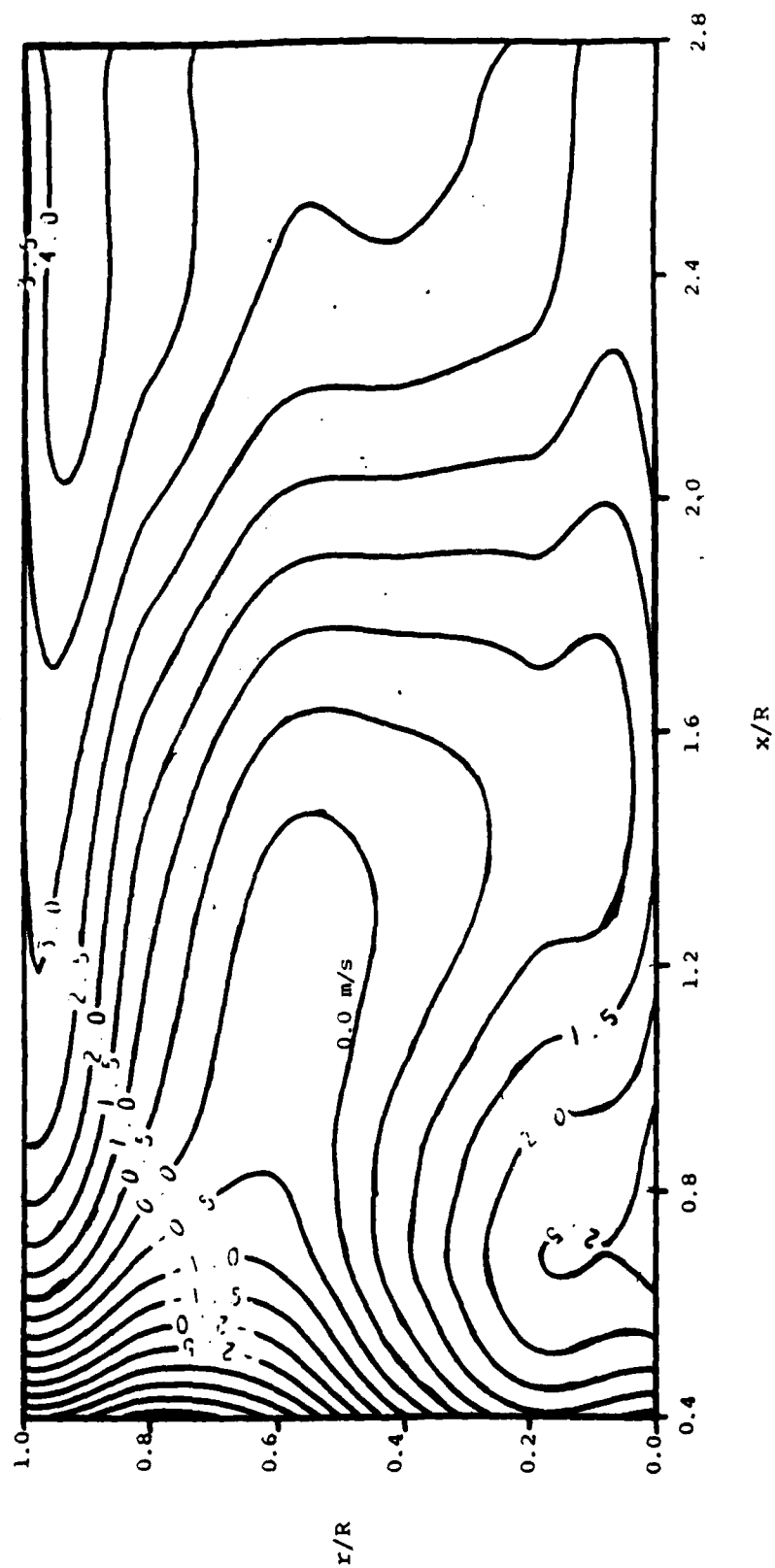


Figure 20. Radial Flame Velocity Profiles for a Propane Flame Operating at a Global Equivalence Ratio of 0.03 and an Air Velocity of 14 m/s.

soot formation rates should be expected. Indeed, this would explain the increase of the soot formation rate and thickness of the flame as the flow rates of both the fuel and air were increased.

Temperature profiles were measured for the three propane flames P11, P22, and P33 and shown in Figures 21, 22, and 23, respectively. Because of the large diameter of the thermocouple used in this experiment (1/4-inch chromel alumel probe), large disturbances of the flow field were observed. The thermocouple probe had to be introduced downstream of the recirculation zone to minimize the disturbances. The maximum temperatures measured in these flames, downstream of the recirculation zone, were of the same order of magnitude. When the flow conditions were increased, the region of maximum temperatures became confined to the centerline and steeper temperature gradients in the radial directions were measured. An increased thickness of the flame, with increased air and fuel flow rates, contributed to higher radiation losses from the soot particles.

The low temperatures measured in these flames are a result of high radiation losses from the thermocouple probe used in this study. A smaller probe with a faster time response will be used in the next phase of this project to interpret adequately the temperature effect on the soot field throughout the formation and oxidation region.

B. 1-BUTENE FLAMES

High sooting rates, obtained with 1-Butene flames, could not be processed properly by the ratio processor. Masks with a small hole at their centers were placed on each set of the receiving optics limiting the number density of the signals reaching the PMTs.

The number mean diameters of the soot particles in all the 1-butene flames studied were found to be comparable (NMD = 0.38 micrometers). Although changes in particle size distribution were observed throughout these flames, they did not exceed the standard deviation (SD = 0.05 micrometers) calculated for each point measurement.

An annular region of maximum soot population density was observed in all the 1-butene flames. The radial location of this region ($0.6 < r/R < 0.8$) was found to vary little with the operating conditions. This region corresponded to the recirculation zone which included separate pockets of fuel and air. The conditions inside these pockets favored soot production. The soot particle population density in butene flames was found to be much higher than for propane flames.

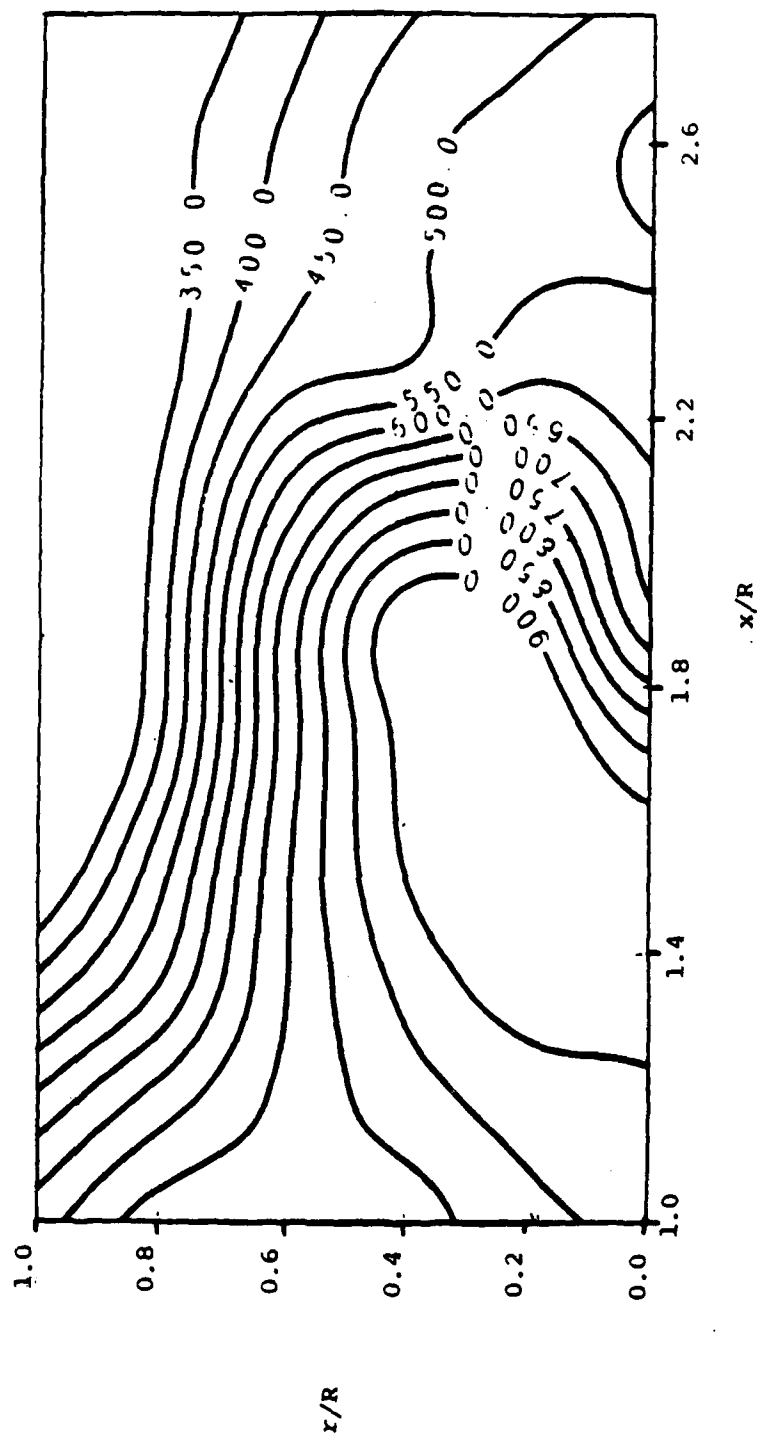


Figure 21. Temperature Profiles (K) for a Propane Flame Operating at a Global Equivalence Ratio of 0.03 and an Air Velocity of 10 m/s.

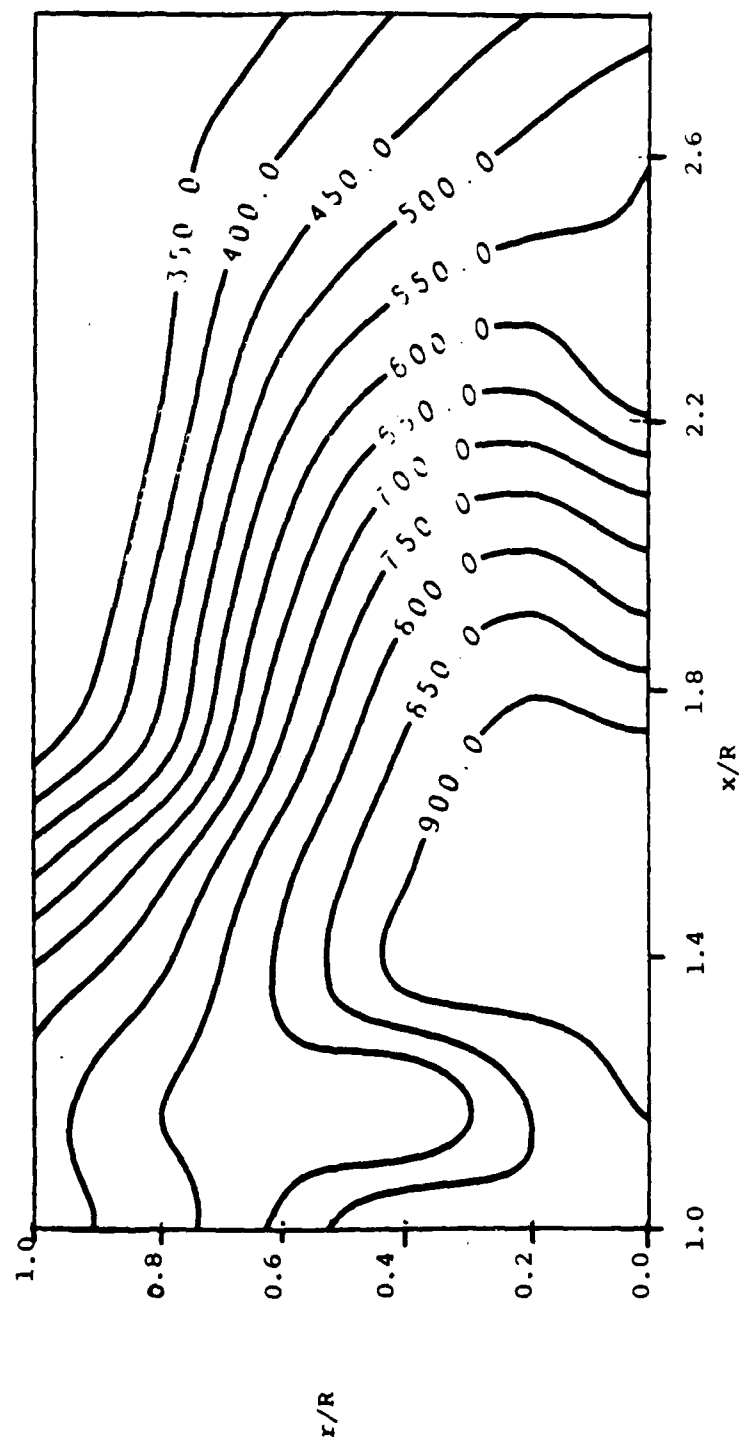


Figure 22. Temperature Profiles for a Propane Flame Operating at a Global Equivalence Ratio of 0.03 and an Air Velocity of 12 m/s.

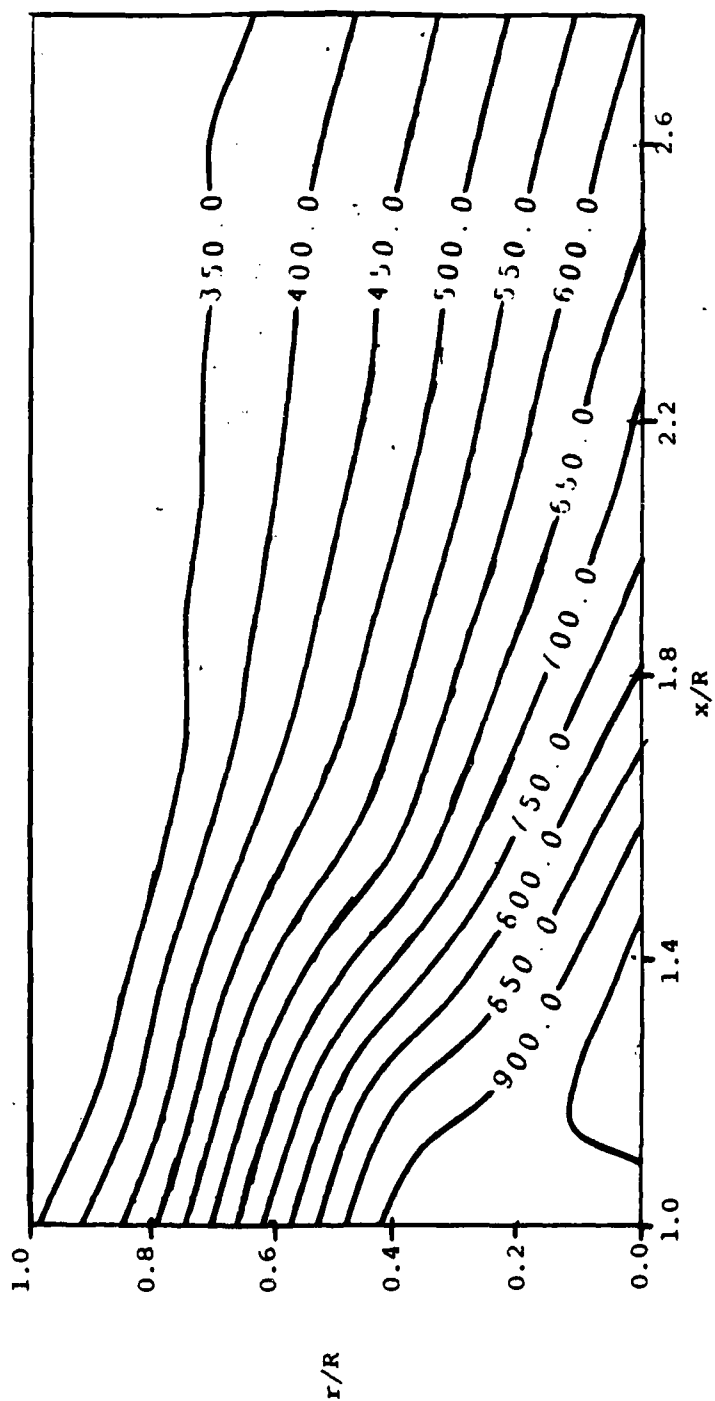


Figure 23. Temperature Profiles for a Propane Flame Operating at a Global Equivalence Ratio of 0.03 and an Air Velocity of 14 m/s.

Figures 24, 25, and 26 show normalized soot particle isoclines for 1-butene flames operating at equivalence ratios of 0.03, 0.04, and 0.05 at a fixed-reference air velocity of 14 m/s. An increase in fuel flow rate at a fixed-reference air velocity resulted in displacement of the soot particle population density toward the face of the burner. Further, an increase of the fuel flow rate resulted in a smaller oxidation region which was the result of higher mixing rate inside the big eddies.

Three 1-Butene flames operating at fixed-reference air velocities of 12 m/s, 14 m/s, and 18 m/s, respectively, at a constant equivalence ratio of 0.03 were investigated to determine the scaling effect on the soot field. The soot field data for the three flames are presented in Figures 27, 24, and 28. An increase in the fuel and air flow rates increased the decay of the soot population density due to better mixing. Further, an expansion of the maximum soot particle density region to the central core of the flame was observed for larger flames.

C. ISOBUTYLENE FLAMES

Similar to 1-Butene flames, isobutylene flames produced high sooting rates that prevented data processing, using fully open collecting optics. The receiving lenses were masked to reduce the scattered light to the PMTs.

The number mean diameter for the isobutylene flames studied was found to be about 0.4 micrometers with a standard deviation of 0.07 micrometers.

Normalized sooting rates for isobutylene flames operating at overall air reference velocities of 10 m/s, 12 m/s, and 14 m/s, respectively, and at an equivalence ratio of 0.03 are presented in Figures 29, 30, and 31. The region of maximum soot particle density was in a zone which included the centerline. The radial diffusion of the soot particles towards the air side was observed to increase with larger flows. Figures 30 and 31, show no noticeable changes in the soot field. This might indicate that the rate of soot formation and oxidation was not affected by higher fuel and air flow rates.

The effect of global equivalence ratios on the soot field was studied, using three isobutylene flames operating at an equivalence ratio of 0.03, 0.04, and 0.05, respectively, and a fixed-air reference velocity of 14 m/s.

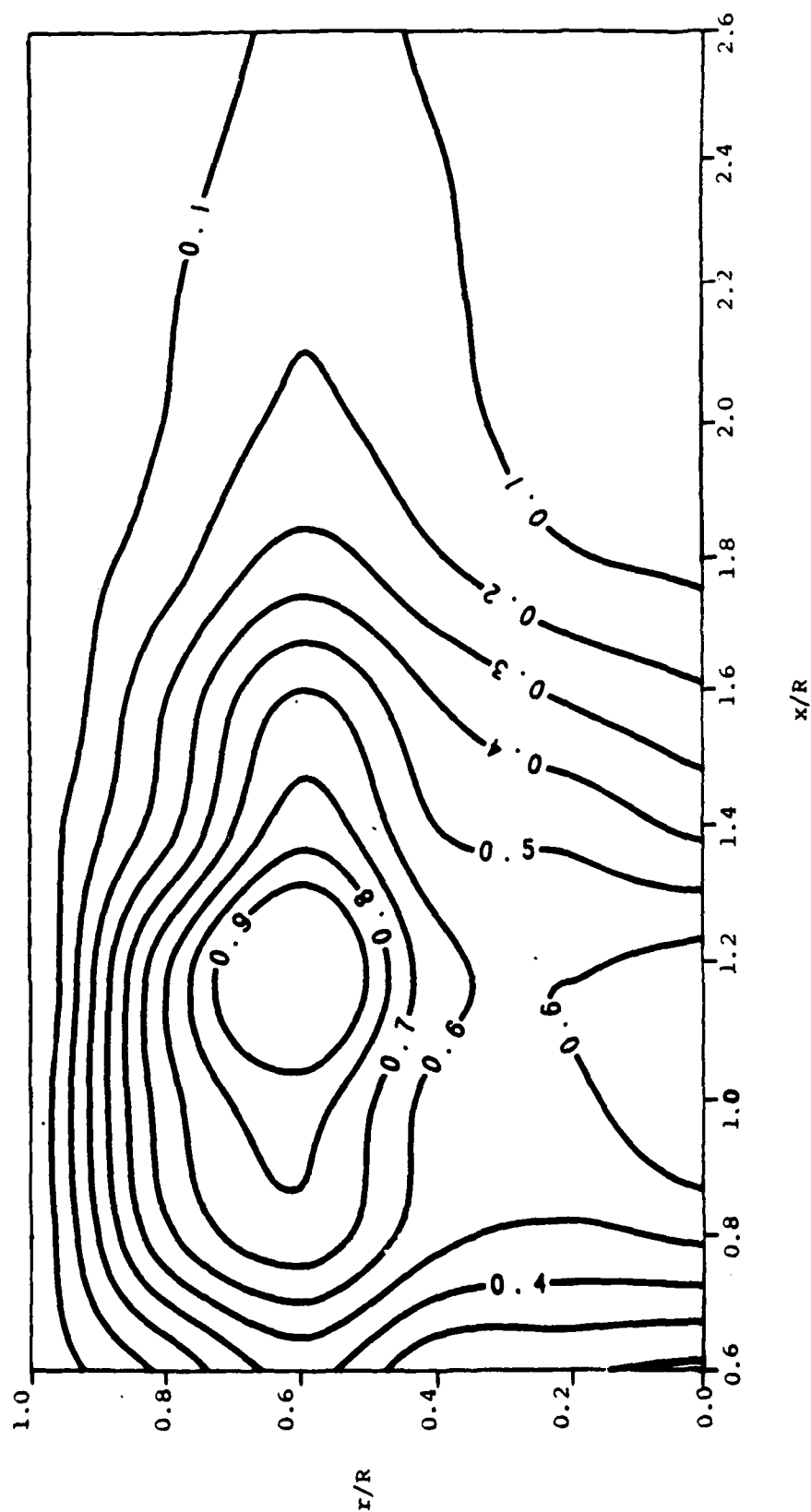


Figure 24. Soot Field Data for 1-Butene Flame Operating at a Global Equivalence Ratio of 0.03 and an Air Velocity of 14 m/s. (The Isoplots are N/N_1 where $N_1=622$ counts/s.)

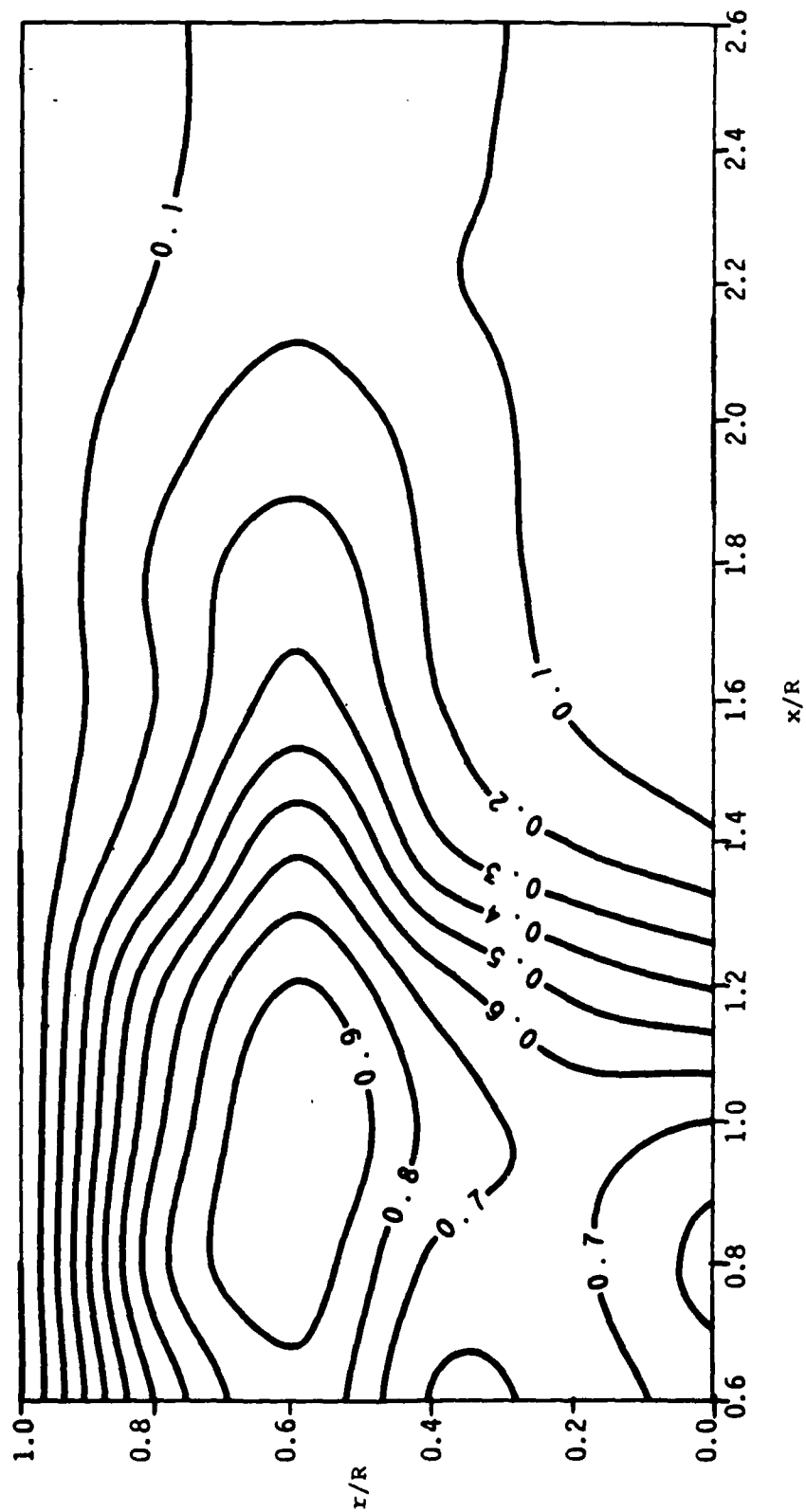


Figure 25. Soot Field Data for 1-Butene Flame Operating at a Global Equivalence Ratio of 0.04 and an Air Velocity of 14 m/s. (The Isoplots are N/N_1 where $N_1=304$ counts/s.)

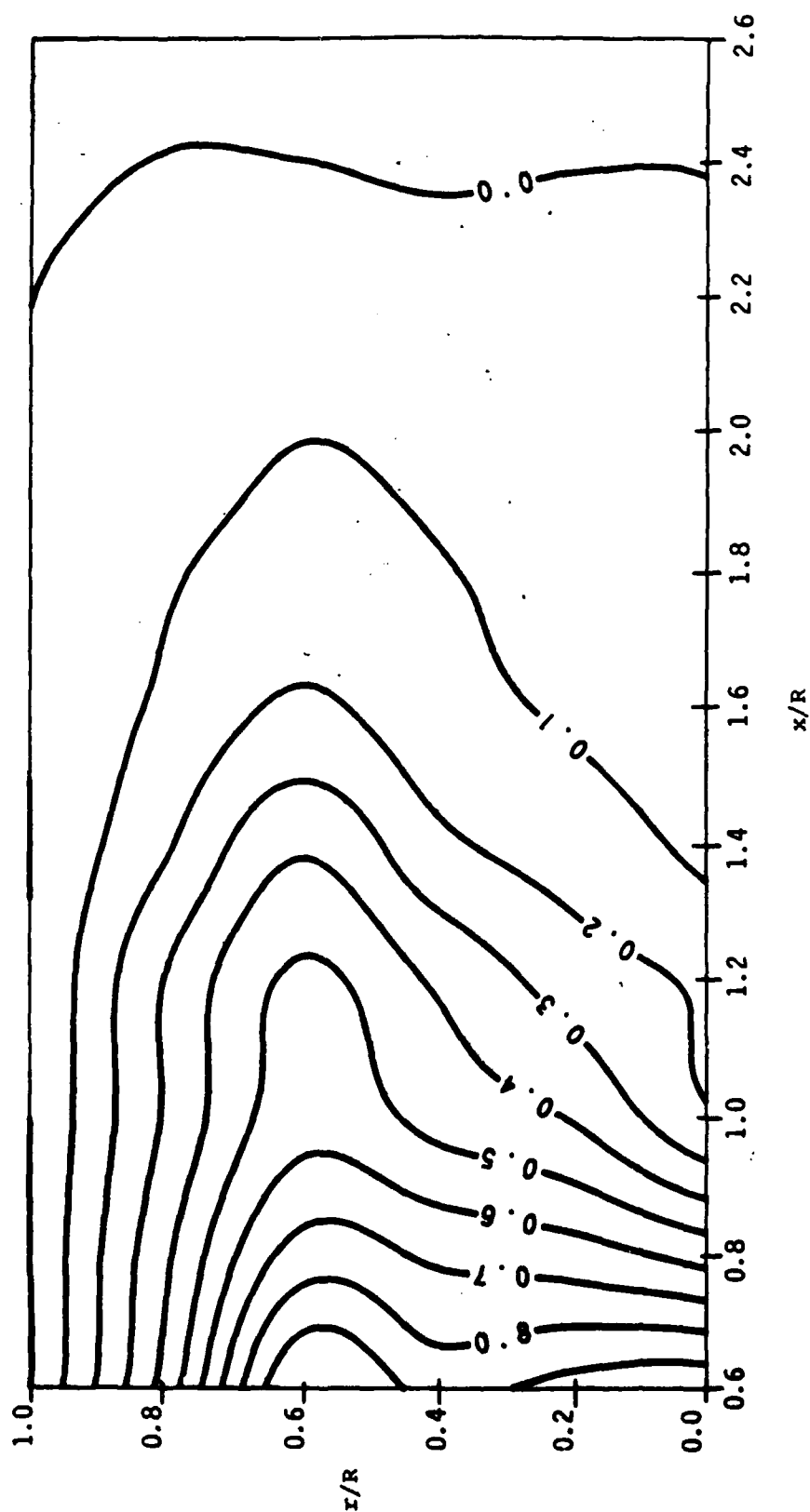


Figure 26. Soot Field Data for 1-Butene Flame Operating at a Global Equivalence Ratio of 0.05 and an Air Velocity of 14 m/s, (The Isoplots are N/N_1 where $N_1=177$ counts/s.)

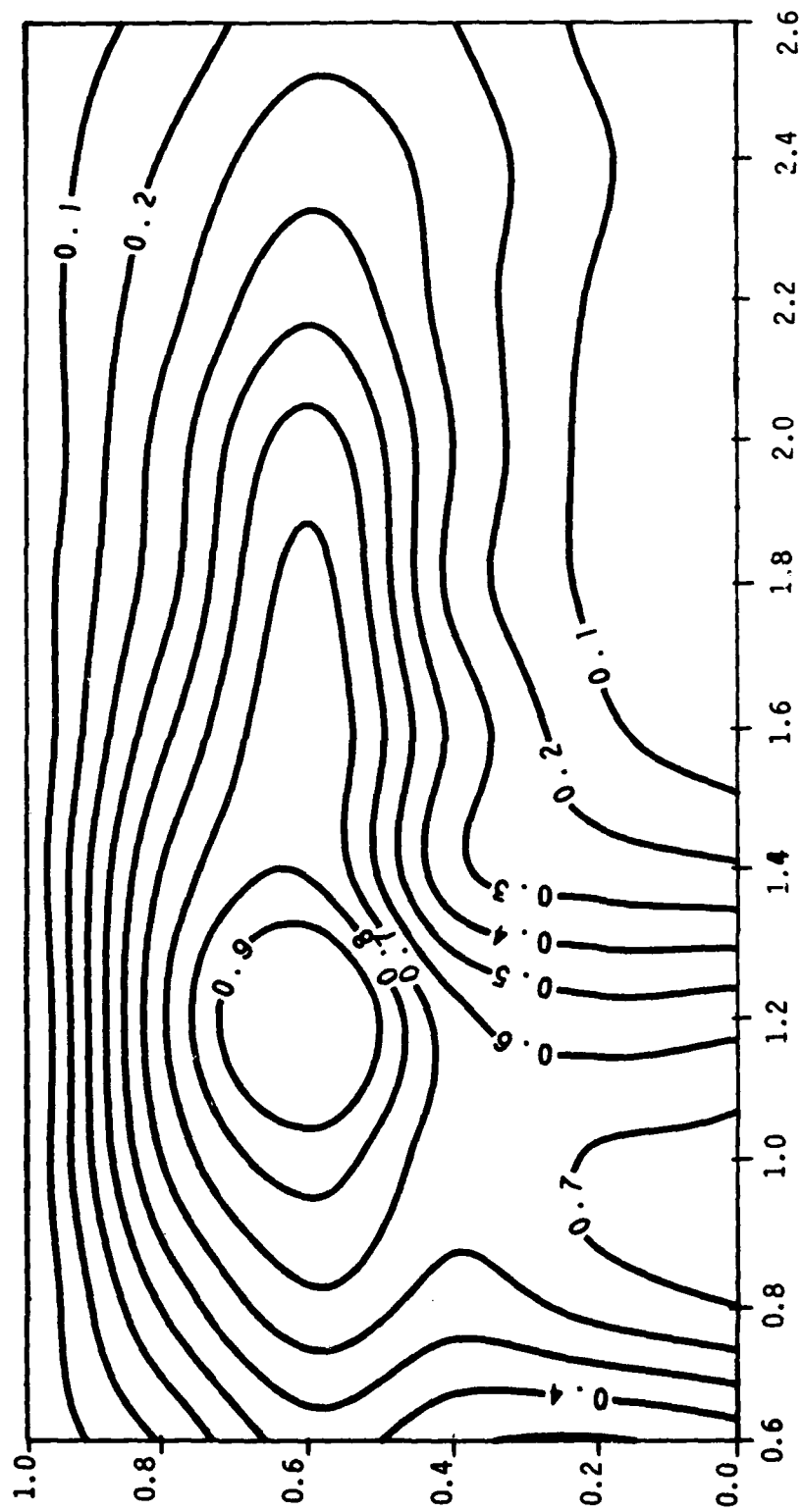


Figure 27. Soot Field Data for 1-Butene Flame Operating at a Global Equivalence Ratio of 0.03 and an Air Velocity of 12 m/s. (The Isoplots are N/N_1 where $N_1 = 308$ counts/s.)

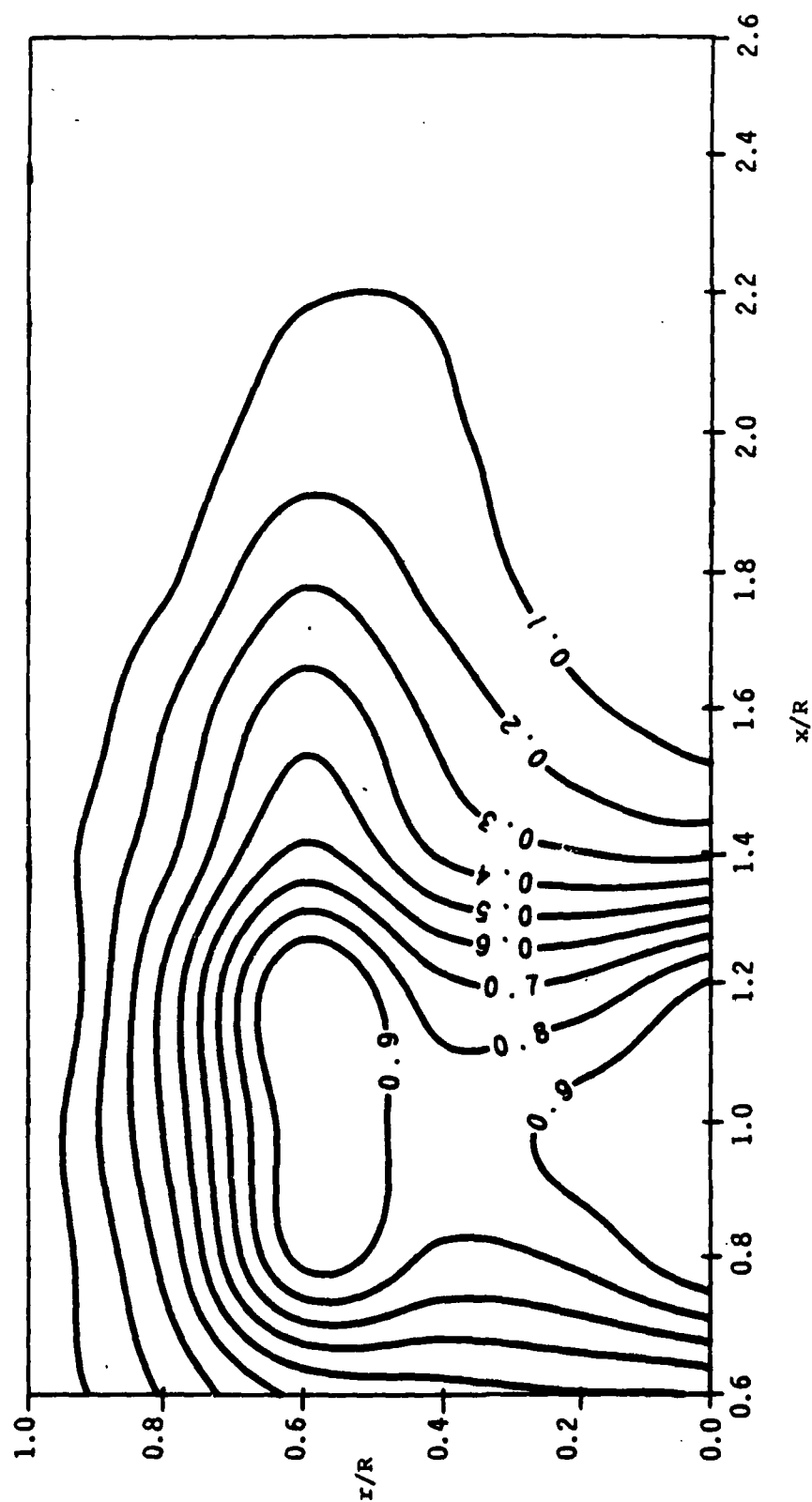


Figure 28. Soot Field Data for 1-Butene Flame Operating at a Global Equivalence Ratio of 0.03 and an Air Velocity of 18 m/s, (The Isoplots are N/N_1 where $N_1=283$ counts/s.)

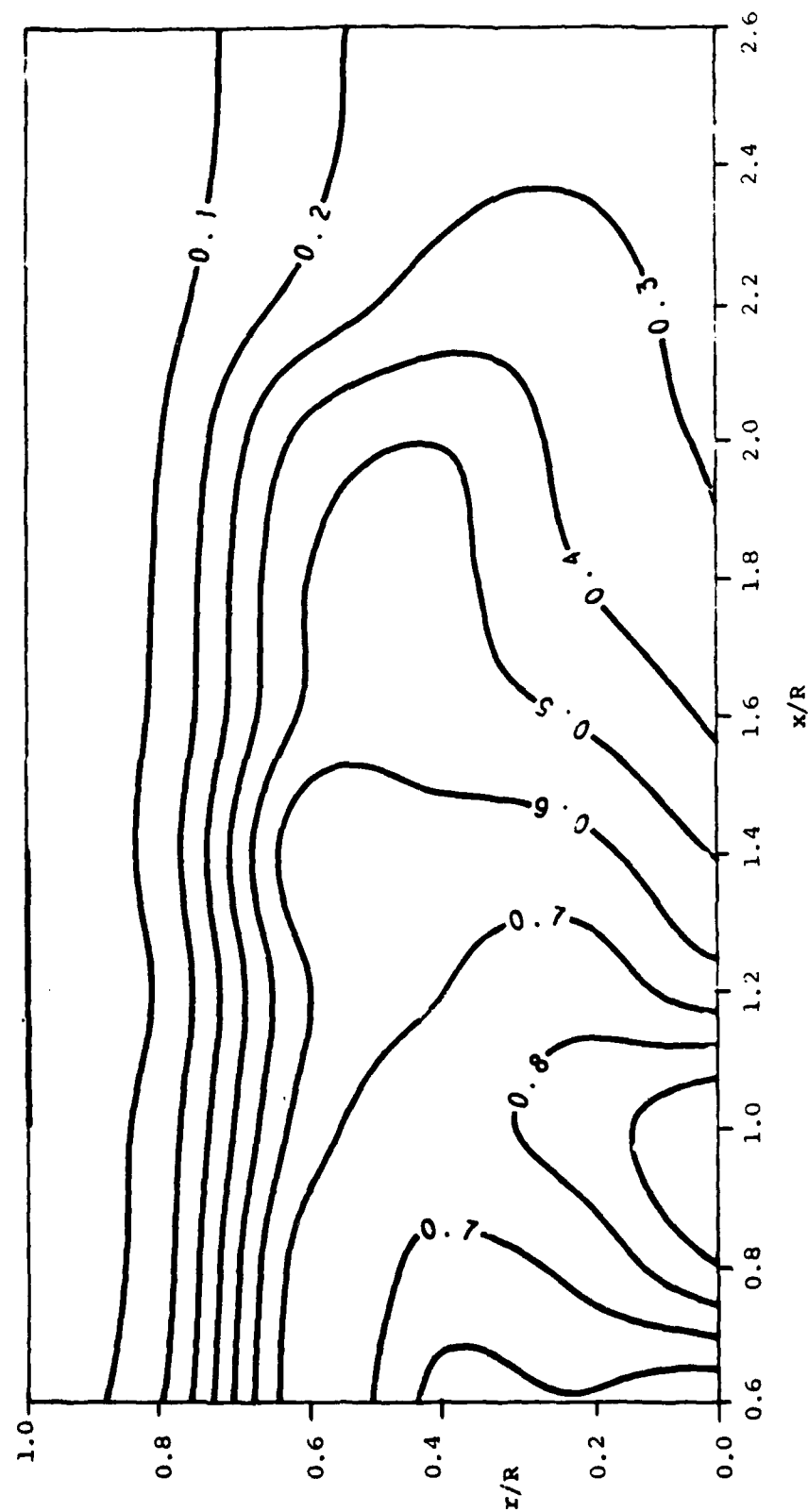


Figure 29. Soot Field Data for an Isobutylene Flame Operating at a Global Equivalence Ratio of 0.03 and an Air Velocity of 10 m/s. (The Isoplots are N/N_1 where $N_1=173$ counts/s.)

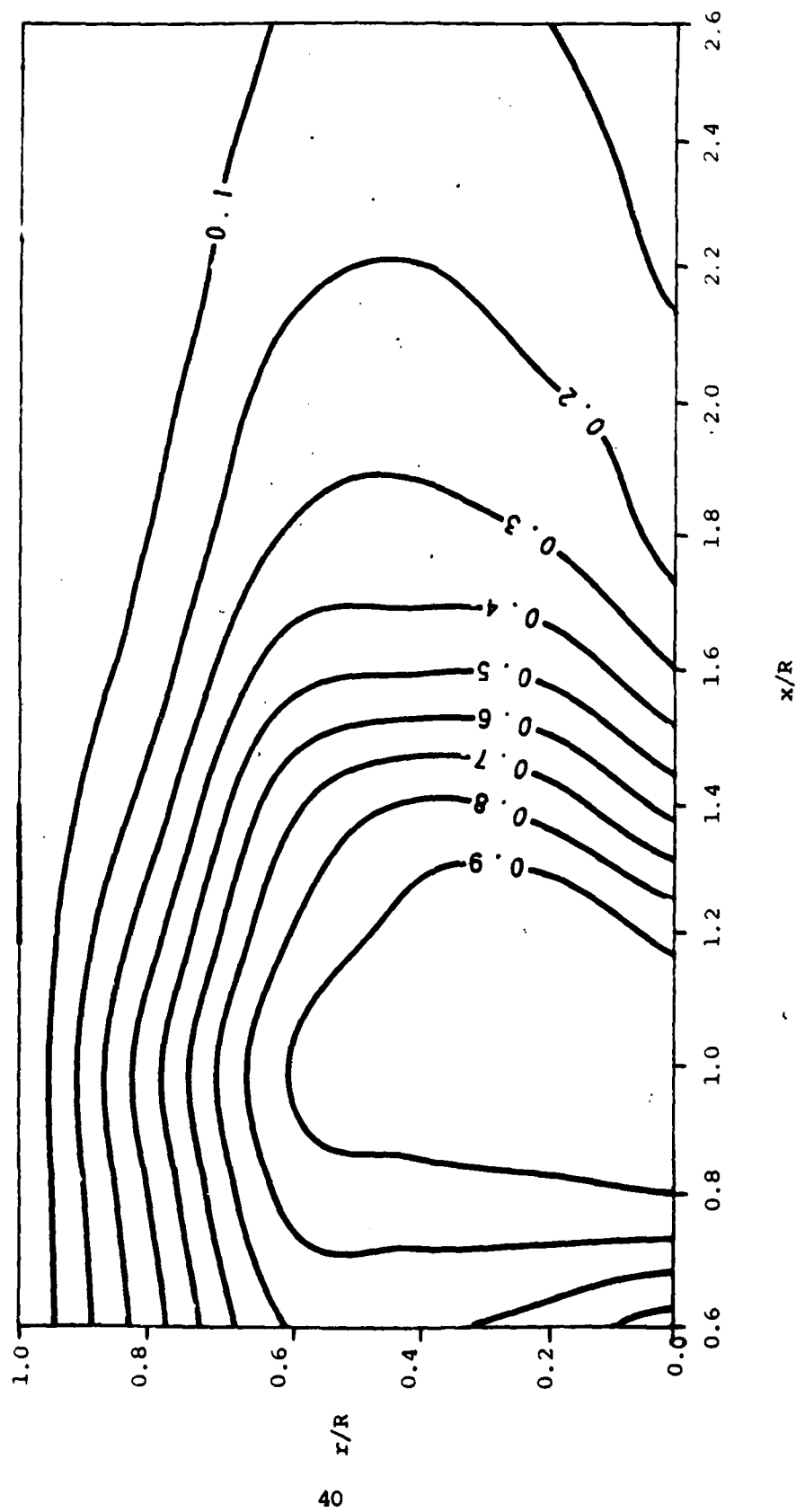


Figure 30. Soot Field Data for an Isobutylene Flame Operating at a Global Equivalence Ratio of 0.03 and an Air Velocity of 12 m/s, (The Isoplots are N/N_1 where $N_1=273$ counts/s.)

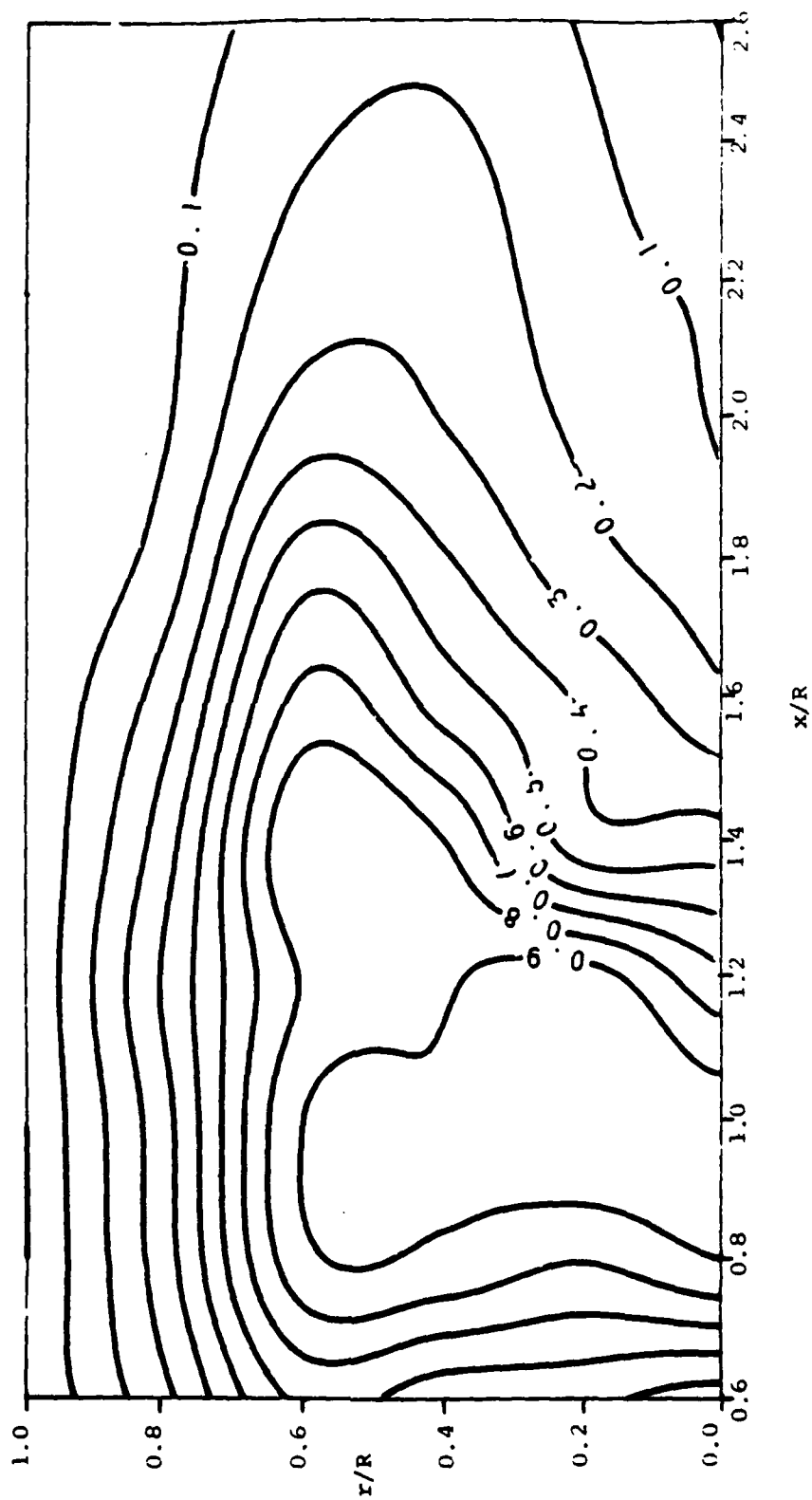


Figure 31. Soot Field Data for an Isobutylene Flame Operating at a Global Equivalence Ratio of 0.03 and an Air Velocity of 14 m/s, (The Isoplots are N/N_1 where $N_1=275$ counts/s,)

The soot field data for the respective flames are presented in Figures 31, 32, and 33. Contrary to propane or 1-butene flames, where an increase of the fuel flow rate at a fixed-reference air velocity had the positive effect of increasing the oxidation rate of the soot particles, in isobutylene flames, an increase of the fuel flow rate for a constant equivalence ratio resulted in an expansion of the soot field region. The soot oxidation rate did not seem to be affected by higher fuel flow rates.

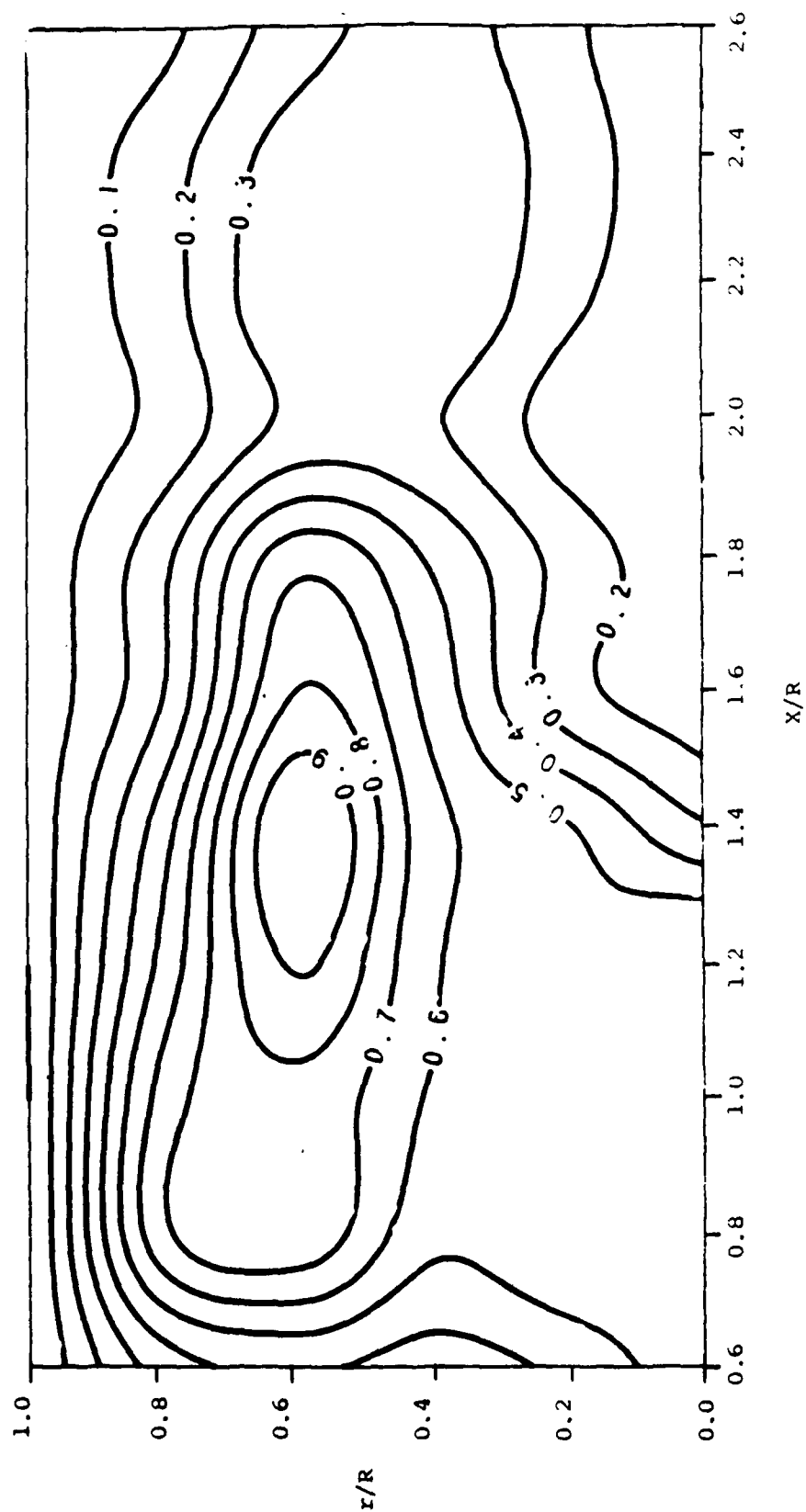


Figure 32. Soot Field Data for an Isobutylene Flame Operating at a Global Equivalence Ratio of 0.04 and an Air Velocity of 14 m/s. (The Isoplots are N/N_1 where $N_1=597$ counts/s.)

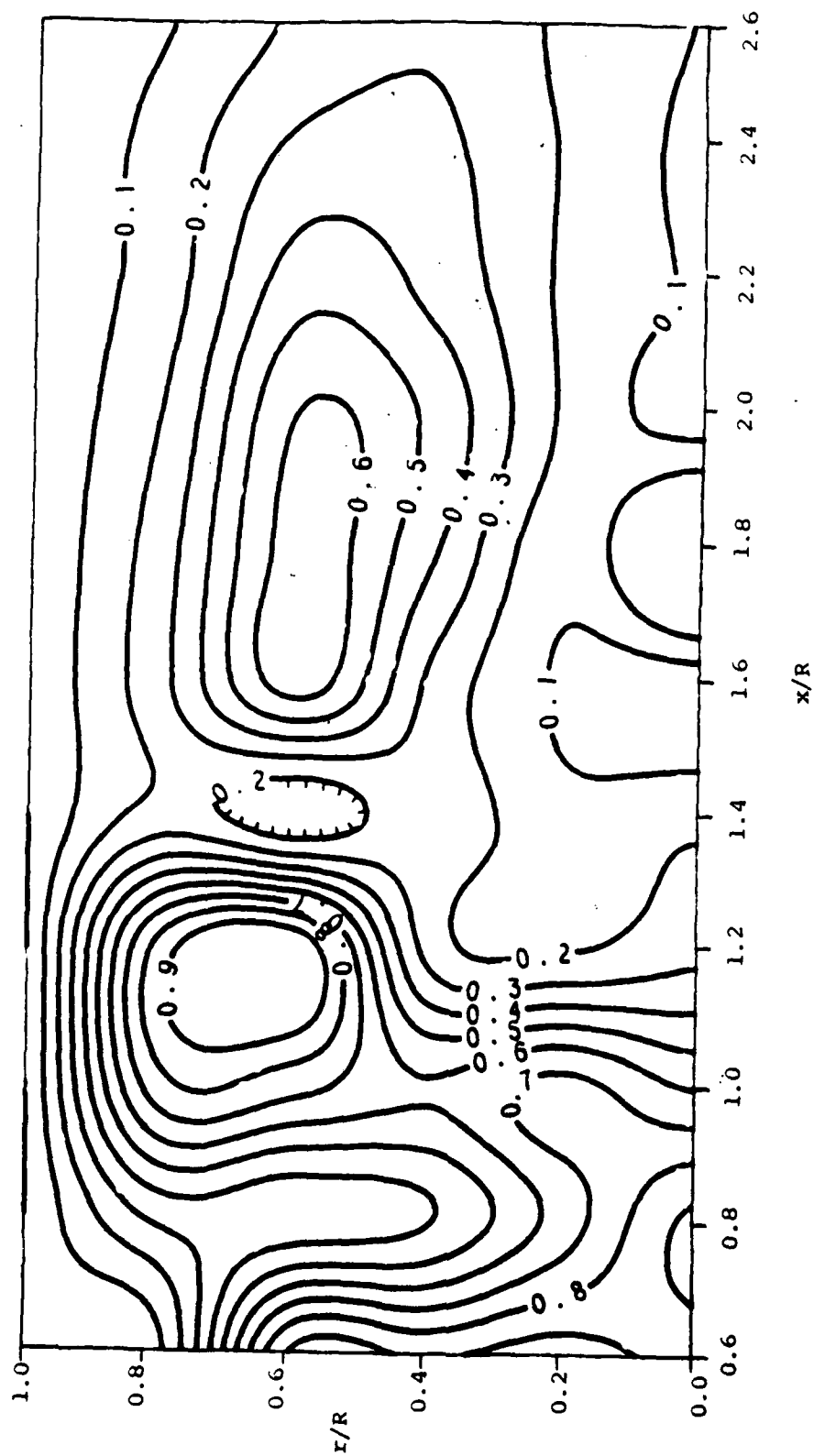


Figure 33. Soot Field Data for an Isobutylene Flame Operating at a Global Equivalence Ratio of 0.05 and an Air Velocity of 14 m/s. (The isoplots are N/N_1 where $N_1=284$ counts/s.)

SECTION IV

SUMMARY AND CONCLUSIONS

A. SUMMARY

This study was designed to establish the different regions of importance in the soot field, and how they are affected by flame aerodynamics, and air/fuel ratio. An optical technique based on the large-angle (40° , 20°) scattered-intensity ratioing technique was used in this study to provide nonintrusive, in situ, real-time point measurements of soot size and population density in the particle size range of 0.12 to 0.57 micrometers.

A bluff body burner was used to generate axisymmetric diffusion flames with recirculating flow fields. Through variation of the operating conditions, the bluff body burner generated flames with different aerodynamic configurations and stability. As a result of this study, the following observations were made:

1. The number mean diameters of the soot particles in all the flames studied were found to vary very little within the limits of the resolvable size range of the optical system. Although changes in the size distribution were observed throughout the flames, these changes did not exceed the standard deviation calculated for each point inside the flames. Only qualitative interpretations of the size distribution in each flame can be made.

2. An annular region of maximum soot particle population density was found inside the recirculation zone located between the fuel jet and the boundaries of the annular air jet. For isobutylene flames, this region included the centerline of the combustor.

3. Dramatic changes in the flame aerodynamic configuration were observed as the operating conditions were varied. These flames changed from a cylindrical to a conical shape as the fuel flow rate was increased and the air velocity maintained constant.

4. For propane and 1-butene flames, the effect of increasing the fuel/air ratio caused an axial displacement of the region of maximum soot population density toward the face of the burner and led to a rapid decay of the soot particle population. However, for isobutylene flames, an increase of the fuel flow rate resulted in an expansion of the soot field.

5. An increase in the fuel and air flow rate for a constant equivalence ratio was observed to increase the decay of the soot particle population rate because of better mixing of the fuel and air. No noticeable changes in the fuel data for isobutylene flames were observed.

6. Introduction of a relatively large physical probe inside the flames disturbed their structure. The temperature measurements made with the 1/4 inch-diameter probe gave only trends of the temperature profiles inside the flames studied.

B. CONCLUSION

The experimental results of this study have shown that the soot field is a strong function of the flame aerodynamics, fuel structure, fuel/air ratio, and flame temperature. The scattered intensity ratioing technique has been proven to be viable in determining the spatial distribution of soot particle size and population density in a hostile environment such as turbulent flames.

The effects of the flame structure on the soot field were positively identified through this study. This information can serve as a data base for comparisons with proposed soot formation models such as the one developed by Magnussen (Reference 1) that takes into account the effects of turbulence on soot formation and combustion.

The chemical structure of the fuels was observed to have some effects on the flame structure. The different heat contents of the fuel provided different combustion temperatures which enhanced or decreased the radiation losses from the soot particles. These variations in temperature eventually affected the soot field data. Meaningful comparisons of the effects of fuel type on soot formation can only be obtained for similar environments (Reference 17). The control of the combustion temperature, flame height, and flame velocities are necessary for such analysis. The adiabatic flame temperature, described by Glassman (Reference 18) as an important parameter in determining the sooting tendency of different fuels, will be investigated in the next project.

REFERENCES

1. Magnussen, B.F., "Modeling of Reaction Processes in Turbulent Flames with Special Emphasis on Soot Formation and Combustion," in Particulate Formation During Combustion, (Sieglä, D.C., and Smith, G.W., ed.) Plenum press, pp. 321, 1980.
2. Farmer, R., Edelman, R.B., and Wong, E., "Modeling Soot Emissions in Combustion Systems," in Particulate Formation During Combustion, (Sieglä, D.C., and Smith, G.W., ed.) Plenum press, pp. 299, 1980.
3. Roquemore, W.M., Bradley, R.P., Stutrud, J.S., Reeves, C.M., and Krishnamurthy, L., "Preliminary Evaluation of a Combustor for use in Modeling and Diagnostics Development," ASME-80-GF93, 25th Annual International Gas Turbine Combustors, New Orleans, Louisiana, 1980.
4. Namazian, M., Kelly, J., Schefer, R.W., and Jonhston, S.C., "Flow and Combustion in a Bluff Body-Stabilized Flame," Presented at the Central/Western Section, The Combustion Institute, paper 2-1B, 1985.
5. Hirleman, E.D., "Optical Technique for Particulate Characterisation in Combustion Environments: The Multiple-Ratio Single Particle Counter," Ph.D Thesis, Purdue University, 1977.
6. Samuelsen, G.S., Wood, C.P., and Jackson, J.A., "Optical Measurements of Soot Size and Number Density in a Complex Flow, Swirl Stabilized Combustor as a Function of Fuel Molecular Structure," NATO AGARD, 62nd Symposium on Combustion Problems in Turbine Engines, Cesme (Turkey), Oct. 1983.
7. D'Alessio, A., "Laser Light Scattering and Fluorescence Diagnostics of Rich Flames produced by Gaseous and Liquid Fuels," in Particulate Formation During Combustion, (Sieglä, D.C., and Smith, G.W., ed.) Plenum Press, pp. 207, 1980.
8. Wood, C.P., Smith, R.A., and Samuelsen, G.S., "Spatially Resolved Measurements of Soot Size and Population in a Swirl-Stabilized Combustor," 20th Symposium (International) on Combustion, the Combustion Institute, 1984.
9. Van de Hulst, H.C., Light Scattering by Small Particles, Dover Pub., New-York, 1981.
10. Kerker, M., The Scattering of Light and other Electromagnetic radiations, Academic Press, New-York, 1981.

REFERENCES
(Concluded)

11. Bohren, C.F., and Huffman, D.R., Absorption and Scattering of Light by Small Particles, John Wiley and Sons, New York, 1983.
12. Santoro, R.J., and Semerjian, H.G., "Soot Formation in Diffusion Flames: Flow Rate, Fuel Species, and Temperature Effects," 20th Symposium (International) on Combustion, the Combustion Institute, pp. 997, 1984.
13. Magnussen, B.F., Hjertager, B.H., Olsen, J.G., and Bhaduri, D., "Effects of Turbulent Structure and Local Concentration on Soot Formation and Combustion in C_2H_2 Flames," 17th Symposium (International) on Combustion, the Combustion Institute, pp. 1383, 1979.
14. Glassman, I., and Yaccarino, P., "Temperature and Fuel Effects in Sooting Diffusion Flames," 18th Symposium (International) on Combustion, the Combustion Institute, pp. 1175, 1981.
15. Kent, J.H., and Wagner, H.G.G., "Temperature and Fuel Effects in Sooting Diffusion Flames," 20th Symposium (International) on Combustion, the Combustion Institute, pp. 1007, 1984.
16. Roper, F.G., "The Prediction of Laminar Jet Diffusion Flame Sizes: Part 1. Theoretical Model," Combustion and Flame 29, pp. 219, 1977.
17. Santoro, R.J., and Semerjian, H.G., "Soot Formation in Diffusion Flames: Effects of Fuel Structure, Temperature and Pressure," AFOSR ISSA 85-0225.
18. Glassman, I., "Phenomenological Models of Soot Processes in Combustion Systems," Princeton University, Department of Mechanical and Aerospace Engineering Report 1450, 1979.